Zootaxa 5128 (4): 451–485
https://www.mapress.com/zt/

Article

ISSN 1175-5326 (print edition)
ZOOTAXA
ISSN 1175-5334 (online edition)

https://doi.org/10.11646/zootaxa.5128.4.1
http://zoobank.org/urn:lsid:zoobank.org:pub:26CA4EF0-61A1-4B60-8C7F-99CA8B8F8700

Vampire Worms; A revision of *Galapagomystides* (Phyllodocidae, Annelida), with the description of three new species

KAILA A. M. PEARSON[1] & GREG W. ROUSE[1, 2*]
[1]*Scripps Institution of Oceanography, University of California San Diego, La Jolla, CA 92093-0202, USA.*
kapearso@ucsd.edu; https://orcid.org/0000-0001-8866-8854
[2]*South Australian Museum, North Terrace, Adelaide SA 5000 Australia.*
**Corresponding author. grouse@ucsd.edu; https://orcid.org/0000-0001-9036-9263*

Abstract

Galapagomystides is an exclusively deep-sea group of Phyllodocidae, originally erected for *Galapagomystides aristata* from hydrothermal vents of the Galapagos Rift. In this study, Phyllodocidae collected from hydrothermal vents and methane seeps from the Pacific Ocean, including specimens from vents of the East Pacific Rise identified as *Galapagomystides* were studied using morphology (light microscopy and scanning electron microscopy) and DNA sequence data. Phylogenetic analysis of the newly generated molecular data (cytochrome c oxidase subunit I, 16S rRNA, 18S rRNA, and 28S rRNA) combined with an already available extensive dataset for Phyllodocidae resulted in a monophyletic *Galapagomystides* comprising five species. *Galapagomystides aristata* was found to occur on the East Pacific Rise vents as well as the Galapagos Rift and is redescribed. Two new species were from hydrothermal vents in the West Pacific, *G. bobpearsoni* n. sp., and *G. kathyae* n. sp., as well as one new species from a cold seep in the eastern Pacific, *G. patricki* n. sp. These new species are formally described, and a previously known vent species, *Protomystides verenae*, is redescribed and transferred to *Galapagomystides*. *Galapagomystides verenae* n. comb. was found to occur in both vents and seeps in the eastern Pacific, from Oregon to Costa Rica. The diagnosis of *Galapagomystides* is amended and the biogeography and habitat evolution of the five species of *Galapagomystides* is discussed.

Key words: new species, hydrothermal vents, methane seeps, cold seeps, Pacific Ocean, Aciculata, Phyllodocida

Introduction

Deep sea chemosynthetic ecosystems (vents and seeps) support diverse faunal communities (Levin 2016; Van Dover 2000). Well-known animals from these habitats tend to be megafauna such as mussels (McCowin *et al.* 2020), clams (Krylova *et al.* 2010) and siboglinid tube worms (McCowin and Rouse 2018). Despite the attention given to larger animals, less conspicuous macrofaunal and meiofaunal groups of annelids, molluscs and crustacea comprise much of the diversity at seeps and vents (Desbruyères *et al.* 2006). Among the annelids, several lineages have diversified, while many clades common in shallow water are rare or absent. Apart from Siboglinidae, diverse annelid groups at vents and seeps include Polynoidae (scale worms), Dorvilleidae, and Hesionidae (Hatch *et al*. 2020; Rouse *et al.* 2018; Yen and Rouse 2020). Other groups such as Serpulidae and Phyllodocidae are present, though with lower species richness (Blake 1985; Rouse and Kupriyanova 2021).

Phyllodocidae is a clade of predatory annelids that contains over 500 named species, found in most marine habitats. Phyllodocidae are commonly known as 'paddle worms', owing to their large, flat dorsal cirri. Many taxa live nearshore in the rocky intertidal (Muir *et al*. 2014), while others live in the deep sea (Imajima 2001). Most Phyllodocidae are benthic, except for the holopelagic group Alciopini (San Martín *et al.* 2021; Rouse *et al.* 2022). Only a few Phyllodocidae have been recorded from chemosynthetic environments, all in the Pacific Ocean. The named species to date are *Galapagomystides aristata* Blake, 1985 from vents at the Galapagos Rift; *Protomystides papillosa* Blake, 1985 from vents at the East Pacific Rise (EPR, at 21°N); *Protomystides hatsushimaensis* Miura, 1988 from a cold seep in Sagami Bay (Japan); and *Protomystides verenae* Blake, 1990 from vents at the Juan de Fuca Ridge (off British Columbia).

Accepted by P. Hutchings: 5 Apr. 2022; published: 22 Apr. 2022

Galapagomystides aristata has been documented within aggregations of Vestimentifera (Govenar *et al.* 2004; Govenar *et al.* 2005) and it has been inferred that *G. aristata* feeds on the blood of Vestimentifera based on anatomical and histological observations of specimens from the East Pacific Rise (Jenkins *et al.* 2002). An unnamed putative *Protomystides* was obtained from both the outside and inside of Vestimentifera tubes and has also been hypothesized to be a 'blood parasite' of Vestimentifera in the Gulf of Mexico (Cordes *et al.* 2007; Becker *et al.* 2013). Kobayashi and Kojima (2017) reported *Protomystides hatsushimaensis* from empty tubes of Vestimentifera as well. While the many members of Hirudinea are blood-feeders and occasionally referred to as vampire worms, it seems appropriate to also apply this common name to *G. aristata* and its blood-feeding relatives.

The first phylogenetic analysis of Phyllodocidae was a morphological cladistic study by Pleijel (1991). The analysis showed that *Galapagomystides* was part of Eteoninae and a sister taxon to a clade comprising *Mysta*, *Hypereteone* and *Eteone*; in addition, Pleijel found that *Protomystides* was a member of Eteoninae. Subsequently there has been no phylogenetic examination of the placement of *Galapagomystides*, though there have been otherwise well-sampled molecular phylogenetic analyses (Eklöf *et al.* 2007; Leiva *et al.* 2018; San Martín *et al.* 2021) comprising many genera within the family, including a member (non-vent) of *Protomystides*.

Here, we present the first molecular sequence data for *Galapagomystides aristata, Protomystides verenae* and several other Phyllodocidae from western Pacific vents and eastern Pacific vents and seeps. This includes fragments of the mitochondrial cytochrome c oxidase subunit I (COI) and 16S rRNA (16S), as well as nuclear 18S rRNA (18S), and 28S rRNA (28S) sequences. These taxa are then analyzed along with available data for other Phyllodocidae. The results require the amendment of *Galapagomystides* to include *Galapagomystides verenae* n. comb., which is redescribed, together with the type species *G. aristata*. In addition, three new species of *Galapagomystides* are formally described.

Materials and Methods

Sample Collection

Sample collection took place over several years in multiple localities shown in Table 1 and Figure 1 during research cruises using ROVs (remotely operated vehicle), or the HOV (human operated vehicle) *Alvin* in the Pacific Ocean during 2005–2019. Samples were fixed in 95% ethanol (for DNA analysis), 5% formalin in seawater (for morphological analysis), or 1% osmium tetroxide (for SEM), and later rinsed and preserved in 50% ethanol for the latter two methods. Some worms were cut in half, with the anterior end fixed in formalin and the posterior fixed in ethanol. Pictures of live specimens were taken in the field, with Leica S8Apo or Leica MZ9.5 stereo microscopes and Canon EOS Rebel cameras. Phyllodocidae samples were collected from vents of the following regions: Lau Back-arc Basin, North Fiji Basin, southern East Pacific Rise (EPR), and the Juan de Fuca Ridge (Oregon). Samples were also collected from seep systems from the following regions: Hydrate Ridge (Oregon), Guaymas Basin (Mexico) and Costa Rica (Pacific), see Figure 1, with locality details in Table 1. Holotypes and paratypes of the three new species and additional material of *G. aristata* and *P. verenae* are deposited at the Benthic Invertebrate Collection at Scripps Institution of Oceanography (SIO-BIC), La Jolla, California, USA. Paratypes of *G. patricki* n. sp. are also deposited at the Museo de Zoología, San José, Costa Rica (MZUCR). Additional material of *G. aristata* is deposited at the South Australian Museum, Adelaide, Australia (SAMA). Paratypes of *G. aristata* and *P. verenae* were borrowed from the Natural Museum of National History (USNM), Smithsonian Institution for morphological study; a single specimen for each species was deaccessioned with permission for scanning electron microscopy and integrated into the SIO-BIC collection (*G. aristata* USNM 081794= SIO-BIC A13574; *G. verenae* new comb. USNM 122686= SIO-BIC A13575).

Morphological Analysis

Preserved specimens were examined using stereo microscopy (Leica MZ9.5), compound light microscopy (Leica DMR HC with differential interference contrast) and scanning electron microscopy (SEM), using a Zeiss EVO10. Parapodia were mounted on slides permanently using 'Aquamount'® [Thermo Fisher Scientific]. Light micrographs were taken with a Canon EOS Rebel T6i camera. For SEM preparation, specimens were dehydrated in an ethanol

TABLE 1. Voucher name, origin, locational coordinate, collection depth, date of collection and GenBank accession numbers of sequenced vouchers and types for COI, 16S rRNA, 18S rRNA, 28S rRNA. Note that *Protomystides verenae* is referred to as *Galapagomystides verenae* n. comb.. * indicates holotype.

Galapagomystides	Voucher	Site	Coordinates	Depth (m)	COI	16S rRNA	18S rRNA	28S rRNA
G. aristata	SIO-BIC A12104	S. East Pacific Rise	23.823° S; 115.456° W	2649	MZ711263	MZ773006	MZ769000	MZ773065
G. aristata	SAMA E8991–E9002	S. East Pacific Rise	23.823° S; 115.456° W	2649	MZ711268-77	-	-	-
G. aristata	SAMA E8989	S. East Pacific Rise	31.863° S; 112.042° W	2334	MZ711266	-	-	-
G. aristata	SAMA E8990	S. East Pacific Rise	31.863° S; 112.042° W	2335	MZ711267	-	-	-
G. aristata	SAMA E8988	S. East Pacific Rise	37.673° S; 110.877° W	2236	MZ711265	-	-	-
G. aristata	SAMA E8987	S. East Pacific Rise	37.673° S; 110.877° W	2236	MZ711264	-	-	-
G. verenae n. comb.	SIO-BIC A1496A	Mound 12, Costa Rica	8.929° N; 84.313° W	1000	MZ711278	-	-	-
G. verenae n. comb.	SIO-BIC A1496B	Mound 12, Costa Rica	8.929° N; 84.313° W	1000	MZ711279	-	-	-
G. verenae n. comb.	SIO-BIC A1830 (A–D)	Jaco Scar, Costa Rica	9.117° N; 84.840° W	1800	MZ711282–85	-	-	-
G. verenae n. comb.	SIO-BIC A1918	Mound 12, Costa Rica	8.931° N; 84.313° W	995	MZ711308	-	-	-
G. verenae n. comb.	SIO-BIC A3263 (A–E)	Guaymas Basin	27.597° N; 111.487° W	1580	MZ711309–13	-	-	-
G. verenae n. comb.	SIO-BIC A1477A	Mound 12, Costa Rica	8.93° N; 84.314° W	1000	MZ711286	-	-	-
G. verenae n. comb.	SIO-BIC A1312	Mound 12, Costa Rica	8.93° N; 84.314° W	1000	MZ711289	-	-	-
G. verenae n. comb.	SIO-BIC A1331	Mound 12, Costa Rica	8.929° N; 84.313° W	1000	-	-	-	-
G. verenae n. comb.	SIO-BIC A8359	Jaco Scar, Costa Rica	9.116° N; 84.840° W	1850	MZ711288	-	-	-
G. verenae n. comb.	SIO-BIC A8379	Jaco Scar, Costa Rica	9.118° N; 84.840° W	1750	MZ711287	-	-	-
G. verenae n. comb.	SIO-BIC A8466	Parrita Seep, Costa Rica	9.031° N; 84.620° W	1400	MZ711290	-	-	-
G. verenae n. comb.	SIO-BIC A8353	Parrita Seep, Costa Rica	9.115° N; 84.836° W	1800	MZ711280	-	-	-
G. verenae n. comb.	SIO-BIC A7991 (A–M)	Juan de Fuca Ridge	45.989° N; 130.027° W	1550	MZ711291–303	MZ773007	MZ769001	MZ773066
G. verenae n. comb.	SIO-BIC A8563 (A–D)	Guaymas Basin	27.589° N; 111.472° W	1690	MZ711304–07	-	-	-
G. verenae n. comb.	SIO-BIC A10044	Jaco Scar, Costa Rica	9.117° N; 84.840° W	1814	MZ711281	-	-	-
G. bobpearsoni n. sp.*	SIO-BIC A4588	Lau Back-arc Basin	20.318° S; 176.137° W	2720	MZ711262	MZ773004	MZ768998	MZ773063
G. bobpearsoni n. sp.	SIO-BIC A4590	Lau Back-arc Basin	21.989° S; 176.568° W	1891	-	-	-	-
G. kathyae n. sp.*	SIO-BIC A13418	North Fiji Basin	16.991° S; 173.915° E	1990	MZ711261	-	MZ768997	MZ773062
G. kathyae n. sp.	SIO-BIC A13422	North Fiji Basin	16.991° S; 173.915° E	1990	-	-	-	-
G. kathyae n. sp.	SIO-BIC A13423	North Fiji Basin	16.991° S; 173.915° E	1990	-	-	-	-
G. kathyae n. sp.	SIO-BIC A13424	North Fiji Basin	16.991° S; 173.915° E	1990	-	-	-	-
G. kathyae n. sp.	SIO-BIC A4651	North Fiji Basin	16.991° S; 173.915° E	1990	-	-	-	-
G. kathyae n. sp.	SIO-BIC A4645	North Fiji Basin	16.991° S; 173.915° E	1990	-	-	-	-
G. kathyae n. sp.	SIO-BIC A4587	Lau Back-arc Basin	20.318° S; 176.137° W	2720	-	-	-	-

.....*Continued on the next page*

TABLE 1. (continued)

Galapagomystides	Voucher	Site	Coordinates	Depth (m)	COI	16S rRNA	18S rRNA	28S rRNA
G. patricki n. sp.*	SIO-BIC A13419	Parrita Seep, Costa Rica	9.030° N; 84.623° W	1415	MZ711314	MZ773005	MZ768999	MZ773064
G. patricki n. sp.	SIO-BIC A13420	Parrita Seep, Costa Rica	9.030° N; 84.623° W	1415	MZ711315	-	-	-
G. patricki n. sp.	SIO-BIC A13421	Parrita Seep, Costa Rica	9.030° N; 84.623° W	1415	MZ711316	-	-	-
G. patricki n. sp.	SIO-BIC A13425	Parrita Seep, Costa Rica	9.030° N; 84.623° W	1415	-	-	-	-
G. patricki n. sp.	SIO-BIC A13426	Parrita Seep, Costa Rica	9.030° N; 84.623° W	1415	-	-	-	-
G. patricki n. sp.	SIO-BIC A13427	Parrita Seep, Costa Rica	9.030° N; 84.623° W	1415	-	-	-	-
G. patricki n. sp.	SIO-BIC A9964	Parrita Seep, Costa Rica	9.032° N; 84.621° W	1400	MZ711320	-	-	-
G. patricki n. sp.	SIO-BIC A9875	Parrita Seep, Costa Rica	9.032° N; 84.621° W	1400	MZ711317	-	-	-
G. patricki n. sp.	SIO-BIC A9877	Parrita Seep, Costa Rica	9.032° N; 84.621° W	1400	MZ711318	-	-	-
G. patricki n. sp.	MZUCR 1510-01	Jaco Scar, Costa Rica	9.118° N; 84.841° W	1762	MZ711319	-	-	-
G. patricki n. sp.	SIO-BIC A9961	Jaco Scar, Costa Rica	9.118° N; 84.840° W	1785	MZ711321	-	-	-
G. patricki n. sp.	SIO-BIC A9934	Jaco Scar, Costa Rica	9.118° N; 84.841° W	1780	-	-	-	-
G. patricki n. sp.	SIO-BIC A1424	off Costa Rica	9.212° N; 84.643° W	805	-	-	-	-

series, transferred to Hexamethyldisilazane (HMDS), and then air dried. Dried specimens were then mounted on aluminum stubs employing double-sided carbon adhesive tabs and tape, and sputter-coated with gold-palladium (Au-Pd).

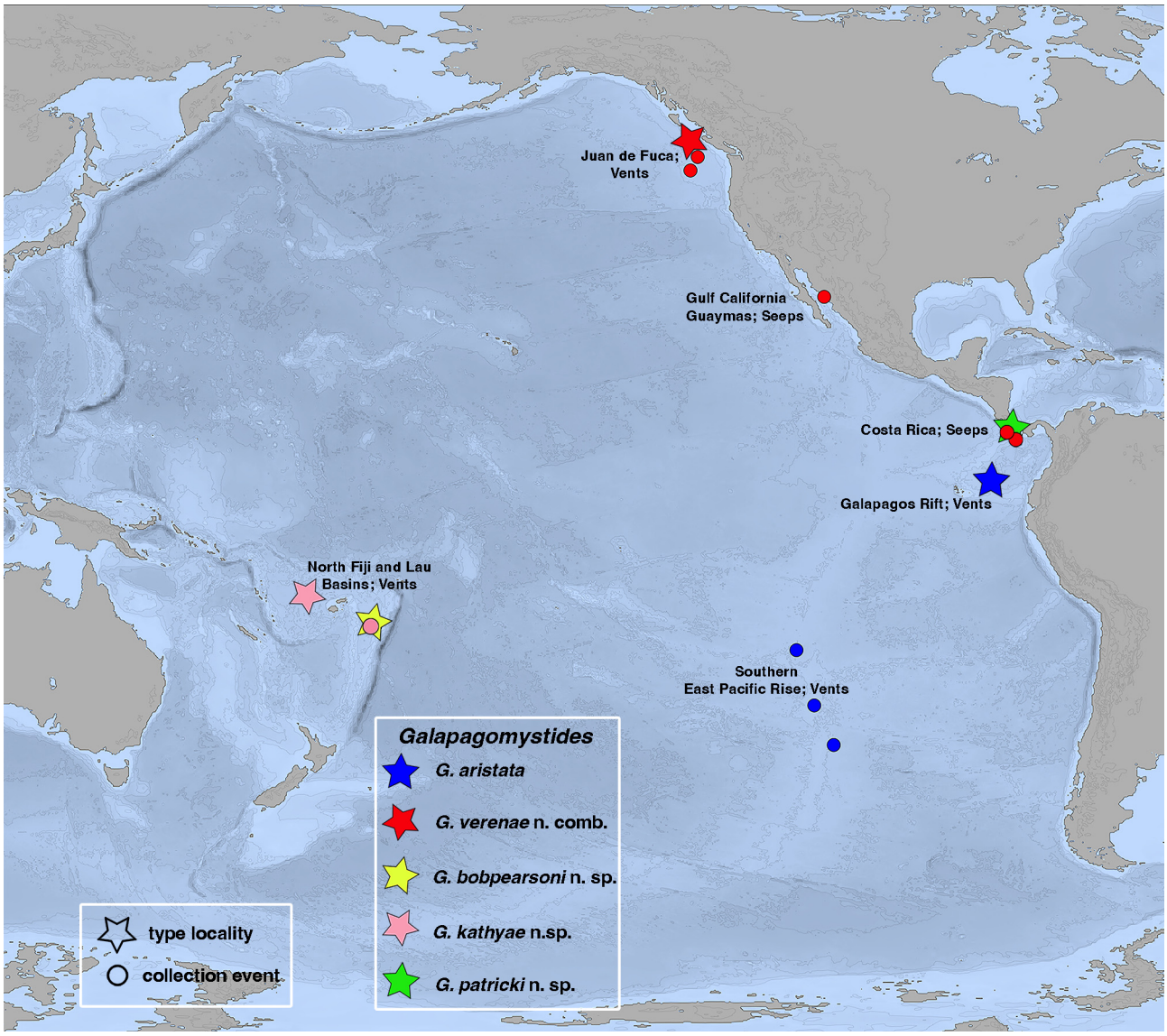

FIGURE 1. Geographic distribution of *Galapagomystides* species, and collection localities (vents and seeps) for this study. Note *G. aristata* was not collected from its type locality Galapagos Rift hydrothermal vents.

DNA Extraction, Amplification, and Sequencing

DNA was extracted from specimens preserved and fixed in 95% ethanol with the Zymo Research DNA-Tissue Miniprep or Microprep kits using the manufacturer's protocol. DNA sequences for mitochondrial cytochrome c oxidase subunit I (COI), 16S rRNA (16S), nuclear 18S rRNA (18S) and 28S rRNA (28S) were amplified using primers as shown in Table 2. PCR amplification was carried out with 12.5 µl Apex 2.0x Taq Red DNA Polymerase Master Mix (Genesee Scientific), 1µl each of the appropriate forward and reverse primers (10µM, 8.5µl ddH_2O, and 2µl eluted DNA and Eppendorf thermal cyclers. Up to 658 base pairs were amplified for COI with a temperature reaction profile as follows: Initial denaturation at 95°C (3 minutes), followed by 40 cycles of denaturation at 95°C (40 seconds), annealing at 42°C (45 seconds), elongation at 72°C (50 seconds), and final extension at 72°C (5 minutes). Up to 506 base pairs were amplified for 16S with a temperature reaction profile as follows: Initial denaturation at 95°C (3 minutes), followed by 35 cycles of denaturation at 95°C (40 seconds), annealing at 50°C (40 seconds), elongation at 72°C (50 seconds), and final extension at 72°C (5 minutes). Up to 1870 base pairs were amplified for 18S with a temperature reaction profile as follows: 18S-1F and 18S-5R, 18S-a2.0 and 18S-9R: Initial

denaturation at 95°C (3 minutes), followed by 40 cycles of denaturation at 95°C (30 seconds), annealing at 50°C (30 seconds), elongation at 72°C (90 seconds), and final extension at 72°C (8 minutes); 18S-3F and 18S-bi: Initial denaturation at 95°C (3 minutes), followed by 40 cycles of denaturation at 95°C (30 seconds), annealing at 52°C (30 seconds), elongation at 72°C (90 seconds), and final extension at 72°C (8 minutes). Up to 1650 base pairs were amplified for 28S with a temperature reaction profile as follows: 28SC1 and 28S1100: Initial denaturation at 95°C (3 minutes), followed by 40 cycles of denaturation at 95°C (40 seconds), annealing at 48°C (45 seconds), elongation at 72°C (50 seconds), and final extension at 72°C (5 minutes); 28S900 and 28S1900: Initial denaturation at 94°C (3 minutes), followed by 35 cycles of denaturation at 94°C (45 seconds), annealing at 52°C (45 seconds), elongation at 72°C (60 seconds), and final extension at 72°C (8 minutes). PCR products were purified using ExoSAP-IT with the manufacturer's protocol (USB, Affymetrix, Ohio). Sanger sequencing was performed by Eurofins Genomics (Louisville, KY). Consensus sequences were assembled using the "De Novo Assembly" option on Geneious v.11.0.5 (Kearse *et al*. 2012) under default settings. All sequences generated for this study were deposited into GenBank (Table 2).

TABLE 2. Primers used for each specified gene, with references.

Gene	Primer Name	Primer Sequence	Source
COI	polyLCO (F)	(5'-GAYTATWTTCAACAAATCATAAAGATATTGG-3')	(Carr *et al.* 2011)
COI	polyHCO (R)	(5'-TAMACTTCWGGGTGACCAAARAA TCA-3')	(Carr *et al*. 2011)
16S	16SarL (F)	(5'-CGCCGTTTATCAA AAACAT-3')	(Palumbi *et al.* 1991)
16S	16SbrH (R)	(5'-CCGGTCTGAACTCAGATCACGT-3')	(Palumbi *et al.* 1991)
28S	28SC1 (F)	(5'-ACCCGCTGAATTTAAGCAT-3')	(Lê *et al.* 1993)
28S	28S1100 (R)	(5'-AGGCATAGTTCACCATCTTTCG-3')	(San Martin *et al.* 2020)
28S	28S900 (F)	(5'-CCGTCTTGAAACACGGACCAAG-3')	(Lockyer *et al.* 2003)
28S	28S1900 (R)	(5'-CCATGTTCAACTGCTGTTCACATG-3')	(San Martin *et al.* 2020)
18S	18S-1F (F)	(5'-TACCTGGTTGATCCTGCCAGTAG-3')	(Giribet *et al.* 1996)
18S	18S-5R (R)	(5'-CTTGGCAAATGCTTTCGC-3')	(Giribet *et al.* 1996)
18S	18S-3F (F)	(5'-GTTCGATTCCGGAGAGGGA-3')	(Giribet *et al.* 1996)
18S	18S-bi (R)	(5'- GAGTCTCGTTCGTTATCGGA-3')	(Whiting *et al.* 1997)
18S	18S-a2.0 (F)	(5'- ATGGTTGCAAAGCTGAAAC-3')	(Whiting *et al.* 1997)
18S	18S-9R (R)	(5'- GATCCTTCCGCAGGTTCACCTAC-3')	(Giribet *et al.* 1996)

Phylogenetic Analyses

New sequence data from this study, along with data for *Endovermis seisuiae* Jimi, Kimura, Ogawa and Kajihara 2020 (Jimi *et al.* 2020) were added to the data set sourced from San Martín *et al.* (2021). The tree was rooted with *Lumbrinereis latreilli* Audouin & Edwards 1833, and other non-Phyllodocidae terminals following San Martín *et al.* (2021). We excluded the COI data for *Lumbrinereis latreilli*, *Glycera dibranchiata* and *Paralacydonia paradoxa* listed by San Martín *et al.* (2021) because these were from the wrong region of COI. Sequences were aligned with MAFFT 7 using the Q-INS-I setting (Katoh and Standley 2013). Aligned sequences for genes COI, 16S, 18S and 28S were concatenated with Sequence Matrix (Vaidya *et al.* 2011). A maximum likelihood (ML) analysis was conducted with RAxML-NG (Kozlov 2019) using RAxML GUI v.2.0 (Edler *et al.* 2021). Bayesian Inference (BI) was also performed using MrBayes 3.2.7 (Ronquist *et al.* 2012). Sequences were partitioned by gene, and the following optimized models were chosen using ModelTest-NG (Darriba *et al*. 2020); 16s: HKY+I+G. 18s: TIM1+I+G. 28s: TIM3+I+G. COI: GTR+I+G. Node support for ML was assessed via thorough bootstrapping (with 1,000 pseudoreplicates).

Uncorrected pairwise distances for COI sequences among the five species studied here were generated with Geneious v.11.0.5. (Table 3). Sequences of the holotypes were used for the three new species. Sequence data from the type locality were used for *G. verenae* that had the minimum distance to any other species and this was also done for the *G. aristata* sequences from the EPR. Haplotype networks using COI data were generated with PopART v.1.7 (Leigh and Bryant 2015) for *G. patricki* n. sp., *G. aristata* and *G. verenae* using the median-joining option (Bandelt

et al. 1999). Habitat (Seep or Vent) and biogeography (East or West Pacific) transformations were generated with Mesquite v.3.61 (Maddison and Maddison 2019) using the most parsimonious transformations and maximum likelihood transformations under the Mk1 model (Lewis 2001).

TABLE 3. Minimum uncorrected pairwise distances for mitochondrial COI among the five species of *Galapagomystides*.

	G. aristata	*G. verenae* n. comb.	*G. bobpearsoni* n. sp.	*G. kathyae* n. sp.	*G. patricki* n. sp.
G. aristata	-				
G. verenae n. comb.	13.1%	-			
G. bobpearsoni n. sp.	14.8%	17.3%	-		
G. kathyae n. sp.	13.1%	14.5%	16.1%	-	
G. patricki n. sp.	17.2%	19.7%	17.8%	17.6%	-

Results

Phylogeny

The ML and BI analyses of the concatenated molecular data were congruent (Fig. 2, most outgroups excluded for space reasons; Fig. 21 shows the results with the outgroup terminals) and matched the results of San Martín *et al*. (2021) with respect to the data they provided. Phyllodocidae fell into two major clades of similar size, marked here as A and B, though neither of these were well supported. The only other new terminal added to the dataset used in San Martín *et al*. (2021) was *Endovermis seisuiae* and this formed a clade with *Paranaitis* spp. (Fig. 2). *Galapagomystides aristata* and the three new species formed a well-supported clade in Clade A along with *Protomystides verenae,* which was sister group to *G. kathyae* n. sp. For this reason, *Protomystides verenae* is referred to as *Galapagomystides verenae* n. comb. *Galapagomystides patricki* n. sp. was the sister taxon to a well-supported clade comprising the remaining *Galapagomystides* species (see **Taxonomy** section). *Galapagomystides kathyae* n. sp. and *G. verenae* were sister taxa with *G. aristata* as sister group to their clade.

Species Delimitation and Haplotype Networks

Uncorrected pairwise distances for the COI sequences (Table 3) showed distances among the five *Galapagomystides* species ranging from 13.1% to 19.7%. The sister group to the *Galapagomystides* clade was *Pterocirrus nidarosiensis*, though with low support (<50% BS and .91 PP). Twelve specimens of *G. aristata* from 1,500 km along the East Pacific Rise were included in the COI haplotype network (Fig. 3), which displayed three distinct haplotypes, varying maximally by only two bases. One haplotype was dominant and occurred in all three sampled locations.

Galapagomystides verenae n. comb. specimens were collected from hydrothermal vents off Oregon, near the type locality, as well as methane seeps off Costa Rica, and the Guaymas Basin (Mexico). The 38 specimens included in the COI haplotype network (Fig. 4) showed 17 different haplotypes over a geographic range of ~6500 km. The maximum intraspecific uncorrected pairwise distance represented across this network was 1.4%. Two of the 17 haplotypes were found across the entire range from Oregon to Costa Rica. This network also shows that *G. verenae* n. comb. is not depth restricted with two haplotypes being found across nearly 1000 m of depth difference.

The eight specimens of *G. patricki* n. sp. included in the COI haplotype network displayed six haplotypes (Fig. 5). These were collected from two localities off Costa Rica that differed in depth by 400 m. The maximum intraspecific uncorrected pairwise distance represented across this network was 2.1%, all from samples at the same site, Parrita Seep, Costa Rica.

Habitat Evolution and Biogeography

The most parsimonious reconstruction for habitat evolution (Fig. 6), shows that the ancestral habitat for *Galapagomystides* could have been either a vent or seep. *Galapagomystides verenae* n. comb. is the only species found to occupy both vents and seeps. Given its phylogenetic placement nested among the seep-dwelling *Galapagomystide*s, the vent-dwelling populations of *G. verenae* would appear to have colonized from a seep habitat.

The most parsimonious reconstruction for the geographical distribution of *Galapagomystides* (Fig. 7) indicates an eastern Pacific origin for the group. There appear to have been two separate colonizations to the western Pacific vents, by *G. kathyae* n. sp. and *G. bobpearsoni* n. sp. respectively.

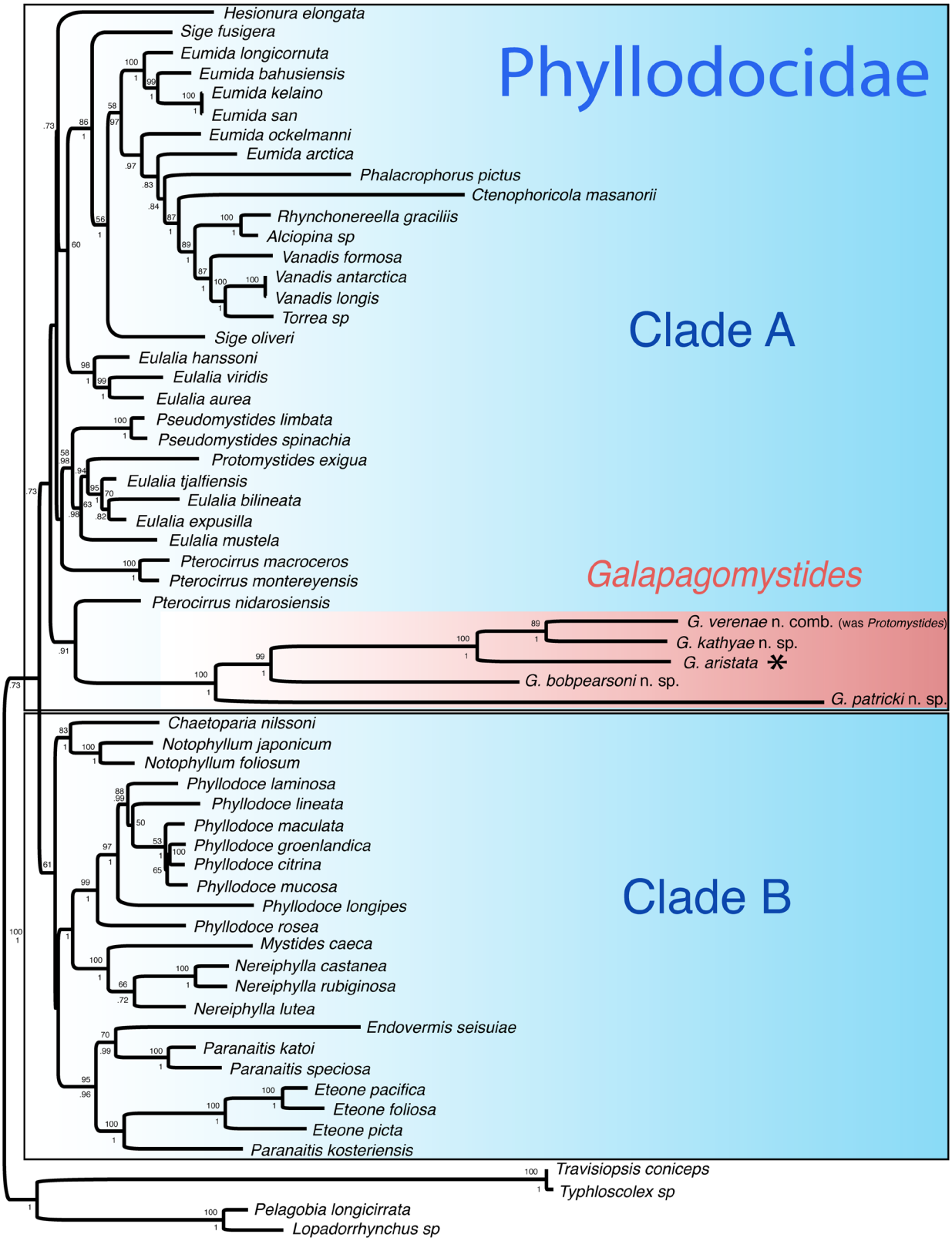

FIGURE 2. Maximum Likelihood (ML) tree generated from the concatenation of mitochondrial (COI 16rRNA) and nuclear genes (18S rRNA, 28S rRNA). Numbers on nodes represent ML bootstrap values (above node) and Bayesian posterior probabilities (below node). Values below 50% for ML and 0.70 for posterior probabilities are not shown. '*' indicates *G. aristata* as the type species of *Galapagomystides*.

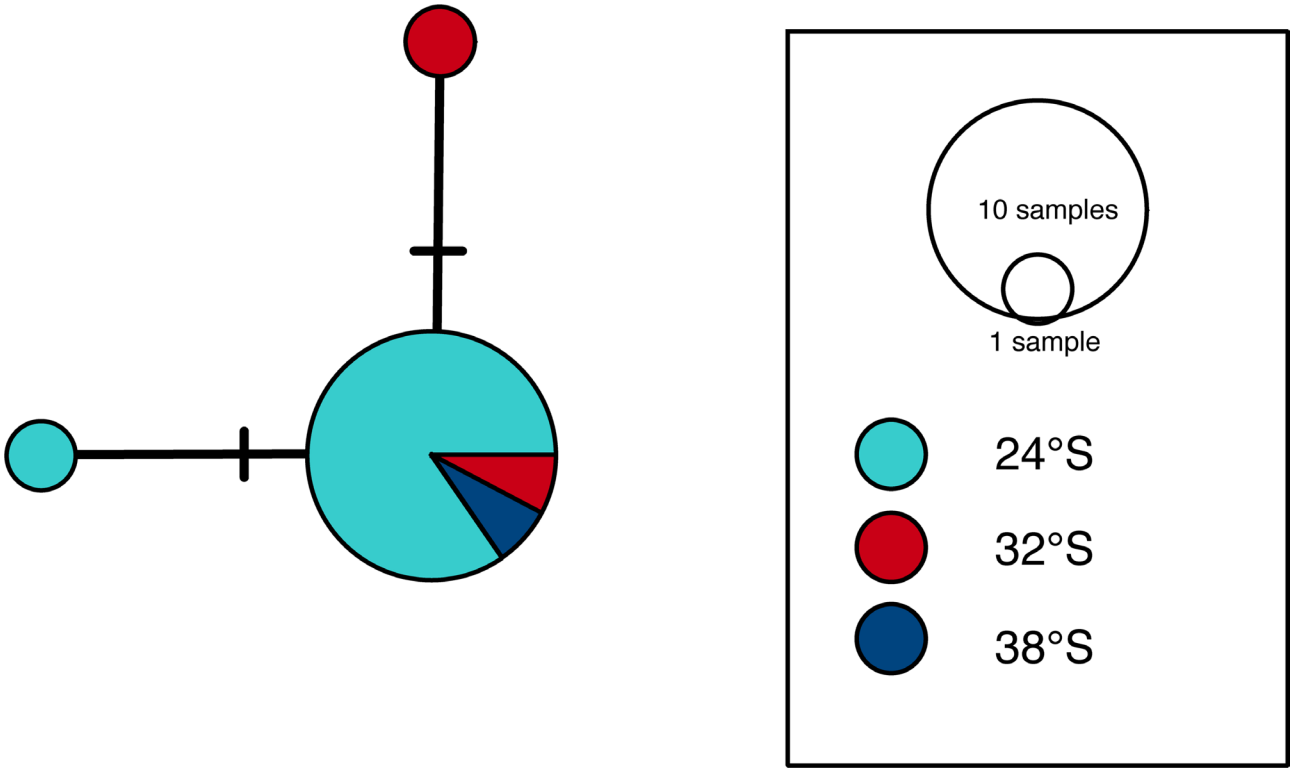

FIGURE 3. *Galapagomystides aristata* haplotype network, based on COI. Specimens were collected from over 1,500 km along the East Pacific Rise.

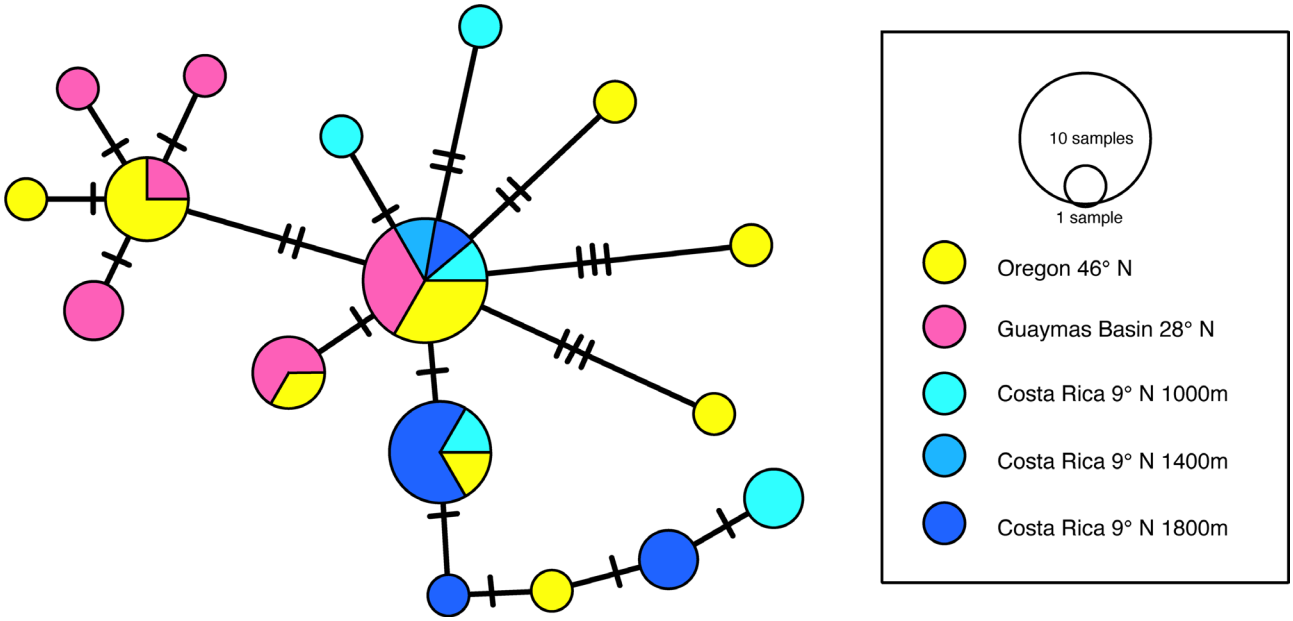

FIGURE 4. *Galapagomystides verenae* n. comb. haplotype network, based on COI. Specimens collected from Costa Rica were sorted into three shades of blue based on varying depth. Oregon is the type locality.

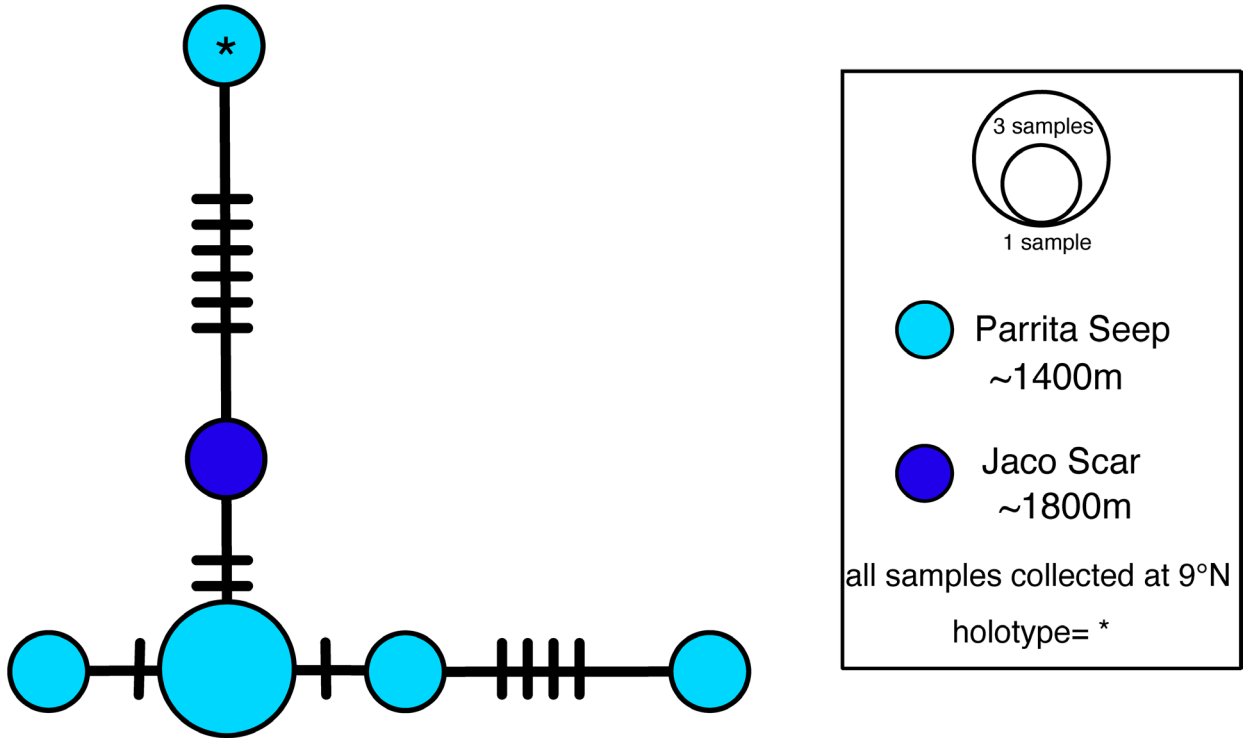

FIGURE 5. *Galapagomystides patricki* n. sp. haplotype network, based on COI. All specimens were collected from Costa Rica at two depths. The haplotype of the holotype is indicated by *.

Taxonomy

Phyllodocidae Ørsted, 1843

Galapagomystides Blake, 1985 (emended)

(Pleijel 1991; Blake 1994)
Table 4.

Type species. *Galapagomystides aristata* Blake, 1985

Diagnosis (emended). Prostomium wider than long. Two antennae; two palps similar in size/shape to antennae. No median antenna or nuchal papilla. Nuchal organs unknown. Eyes absent. Smooth proboscis, papillae at distal end. Segment 1 fused or not (dorsally) to prostomium. Segment 1 distinct ventrally. Elongated dorsal cirri (EDC) (= tentacular cirri) on segments 1, 2; EDC on segment 3. No ventral cirri on segment 1. Ventral cirri on segment 2 elongated or like following segments. Parapodia uniramous, notopodial chaetae absent. Neuropodium with central fascicle containing compound chaetae; one simple emergent acicula. Compound chaetal shaft cylindrical; pointed blade extended from falcate joint. Rostrum of chaetal shaft asymmetrical/hooked. Presence of segmental bands of cilia. Pygidial cirri robust ellipsoid lobes. Living animals are red.

Remarks. Based on this study, *Galapagomystides* now includes five species; *G. aristata*, *G. bobpearsoni* n. sp., *G. kathyae* n. sp., *G. patricki* n. sp., and *G. verenae* n. comb. Blake's (1985) original *Galapagomystides* diagnosis stated that the genus has segment 1 fused dorsally to the prostomium, and no dorsal cirri on segment 3. We amend the *Galapagomystides* diagnosis to allow for the variation shown in other members of the genus. For instance, some taxa do not have segment 1 fused to the prostomium and may have dorsal elongated cirri on segment 3 in addition to segments 1 and 2 (Table 4). Pleijel's (1991) diagnosis of *Galapagomystides* accepted Blake's (1985) diagnosis, with the addition of nuchal organs present as dorso-lateral ciliated pits between the prostomium and segment 1. Pleijel (1991) also questioned the presence of segmental ciliated bands though their presence is confirmed here. All species within *Galapagomystides* have an asymmetrical/hooked tip of the chaetal shaft, which is unique to the genus among Phyllodocidae. For a morphological summary of variation within *Galapagomystides* see Table 4.

TABLE 4. Features of *Galapagomystides* species. (P) = present. (A) = absent.

	elongated dorsal cirri segment			**elongated ventral cirri** segment			**segment 1 fused to prostomium**
Taxon	**1**	**2**	**3**	**1**	**2**	**3**	
G. aristata	P	P	A	A	P	A	P
G. verenae n. comb.	P	P	P	A	P	A	A
G. bobpearsoni n. sp.	P	P	P	A	P	A	P
G. kathyae n. sp.	P	P	P	A	P	A	P
G. patricki n. sp.	P	P	A	A	A	A	A

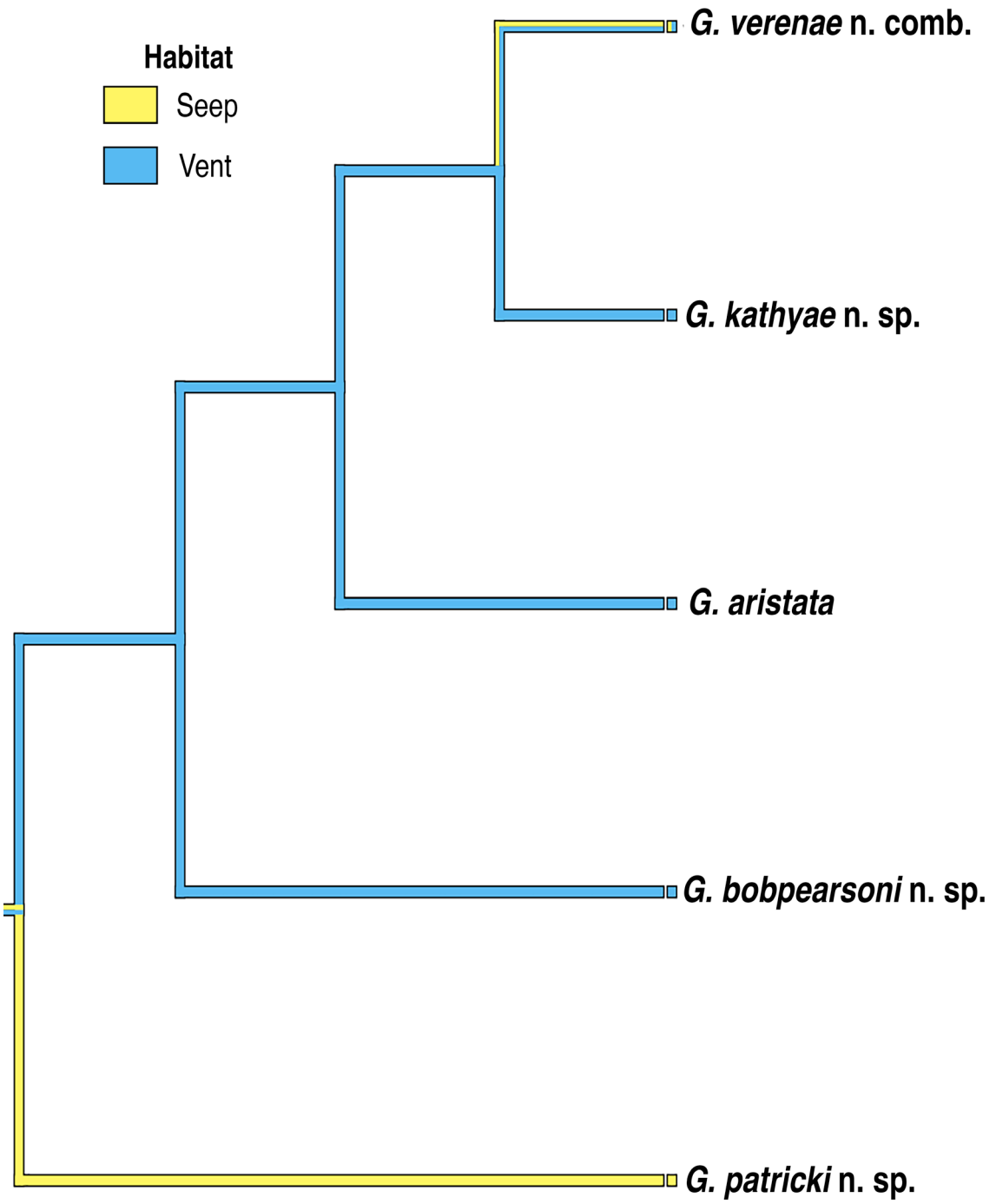

FIGURE 6. Most parsimonious reconstruction for habit of *Galapagomystides*. The ancestral state for the clade is ambiguous and could have been seep or vent. *Galapagomystides verenae* n. comb. is found at both vents and seeps and appears to have colonized seeps from a vent ancestral habitat.

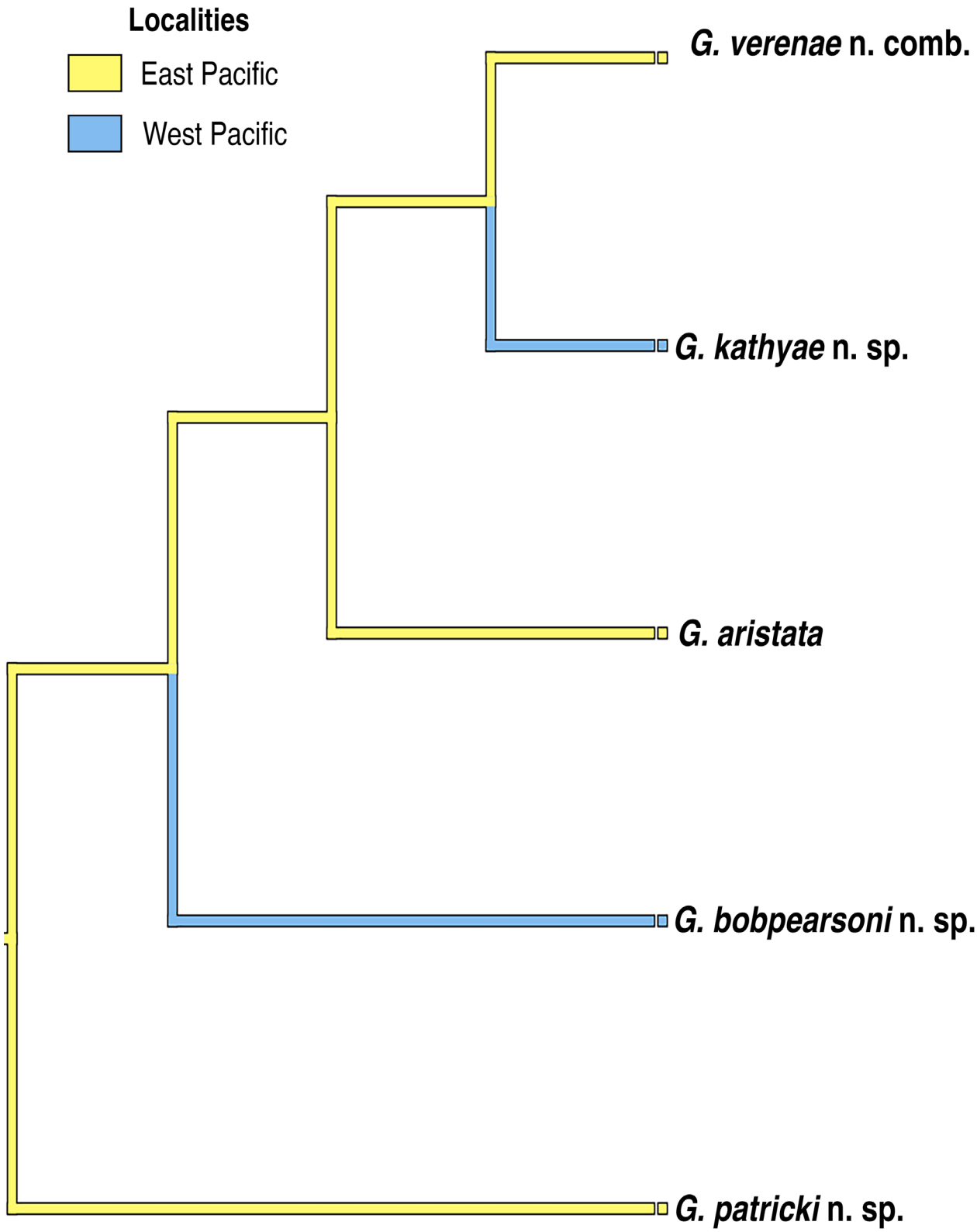

FIGURE 7. Most parsimonious reconstruction for Pacific habitat of *Galapagomystides*. The ancestral state for the clade is the eastern Pacific with *Galapagomystides bobpearsoni* n sp. and *G. kathyae* n. sp. independently colonizing the western Pacific.

***Galapagomystides aristata* Blake 1985**
Figures 8–10

Blake (1985:69, 71-73), Blake (1994: 119), Desbruyères *et al*. (1997: 80), Desbruyères *et al*. 2006: 216), Dreyer (2004: 55, 58, 60. 62), Gollner *et al*. (2015: 62), Govenar *et al*. (2004:179), Govenar *et al*. (2005:71, 72, 75), Govenar *et al*. (2007: 7-9, 11), Jenkins *et al*. (2002: 243, 245, 249-252), Rodrigo *et al*. (2015: 100), Tunnicliffe (1992: 340), Tunnicliffe *et al.* (1998: 367), Van Dover (2002: 145, 146, 148).

Diagnosis. First segment fused dorsally to prostomium. Elongated dorsal cirri on segments 1 and 2. Elongated ventral cirri on segment 2. Exaggerated hook-like joint of compound chaetae.

Material Examined. SIO-BIC A13574 (paratype transferred from USNM, used for SEM), Galapagos Rift Geothermal Vents, ~2,500 m depth; SIO-BIC A12104*, SAMA E8987*, SAMA E8988*, SAMA E8989 *, SAMA E8990*, SAMA E8991–E9002*, southern East Pacific Rise, ~2,200–2,700 m depth. For locality details see Table 1. * indicates sequenced specimens.

Description. Up to 22 mm long, 1 mm wide at segment 10 for ~100 segments. Body semi-translucent and white at parapodial lobes, dorsal and ventral cirri, elongated cirri, pygidial cirri, prostomium and pygidium; deep pink/red in longitudinal center in life (Fig. 8A–D). Body brown/orange with numerous dark pigmentation speckles in preserved (formalin/ethanol) state (Fig. 8E). Rounded, lobe-like prostomium; nuchal organs not visible. Anterior dorsal edge of prostomium with paired cylindrical antennae ~0.2 mm long (Fig. 9C). Paired palps ventral to antennae, similar in shape and length to antennae (Fig. 9C). Segment one dorsally fused to prostomium, following segments clearly demarcated (Fig. 9A, C, E). Pair of elongated dorsal cirri [tentacular cirri] on each of segments 1 (~0.25 mm long), 2 (~0.28 mm long) (Fig. 9A, C). All elongated dorsal cirri cirriform, tapering distally. Pair of elongated ventral cirri on segment 2 (~0.2 mm long) (Fig. 9A, C). Conical, tapering regular ventral cirri (~0.08 mm long) begin on segment 3 continuing posteriorly (Fig. 9C). Bulbous, rounded dorsal cirri (~0.08 mm long) begin on segment 4 continuing posteriorly (Fig. 9A). Dorsal cirri absent on segment 3 (Fig. 9A). Parapodia uniramous, notopodial chaetae absent; neuropodium with central fascicle containing ~5–8 compound chaetae; one simple emergent acicula (Figs 8F, H, 10B, D, E). Compound chaetal shaft cylindrical; thin, flattened pointed blade extended from curved joint (Figs 9D, 10B, D, E). Pygidium with one pair of cirriform pygidial cirri tapering distally (~0.2 mm long) (Fig. 9B). Proboscis protrudes ¼ body length, smooth until ½ distance distal, then lined with papillae (Fig. 9E).

Variation. There was a very slight variation in animal length and number of segments in comparison to the original description (Blake 1985). The specimens studied here reached ~100 segments and a total length of 22 mm (Fig. 8E) as opposed to ~90 segments and a total length of 20 mm described by Blake (1985). All other characters match the original description.

Remarks. The *G. aristata* samples used in our DNA analyses were collected along the EPR, over 3,000 km from the type locality (= Galapagos Rift). However, the specimens matched Blake's description and the examined paratype closely. Previous authors have recorded *G. aristata* specimens from the EPR, though these were not taxonomic studies (Jenkins *et al.* 2002; Govenar *et al.* 2004; 2005). Here we extend the range of *G. aristata* to the EPR, though final confirmation requires DNA sequencing of *G. aristata* from the Galapagos Rift vents. Unique features of *G. aristata* shared between specimens used in this study and the paratypes include the hook-like joint of the compound chaetae (Figs 9D, 10D), fusion of segment one dorsally but not ventrally to the prostomium (Figs 9A, C, 10A, C), the prostomium size and shape (Figs 9A, C, 10A, C).

Galapagomystides aristata is morphologically most like *G. kathyae* n. sp. and *G. bobpearsoni* n. sp. in that all have segment 1 dorsally fused to the prostomium. However, in the phylogenetic analyses, *G. aristata* was found to be the sister group to a clade comprising *G. kathyae* n. sp. and *G. verenae*. *Galapagomystides aristata* has a smooth proboscis as mentioned in previous descriptions (Blake 1985; Pleijel 1991), though there are papillae located at the distal third of the proboscis (Fig. 9E). Pleijel's (1991) diagnosis of *Galapagomystides* claimed nuchal organs present as dorso-lateral ciliated pits between the prostomium and segment 1, however nuchal organs were not located in this study.

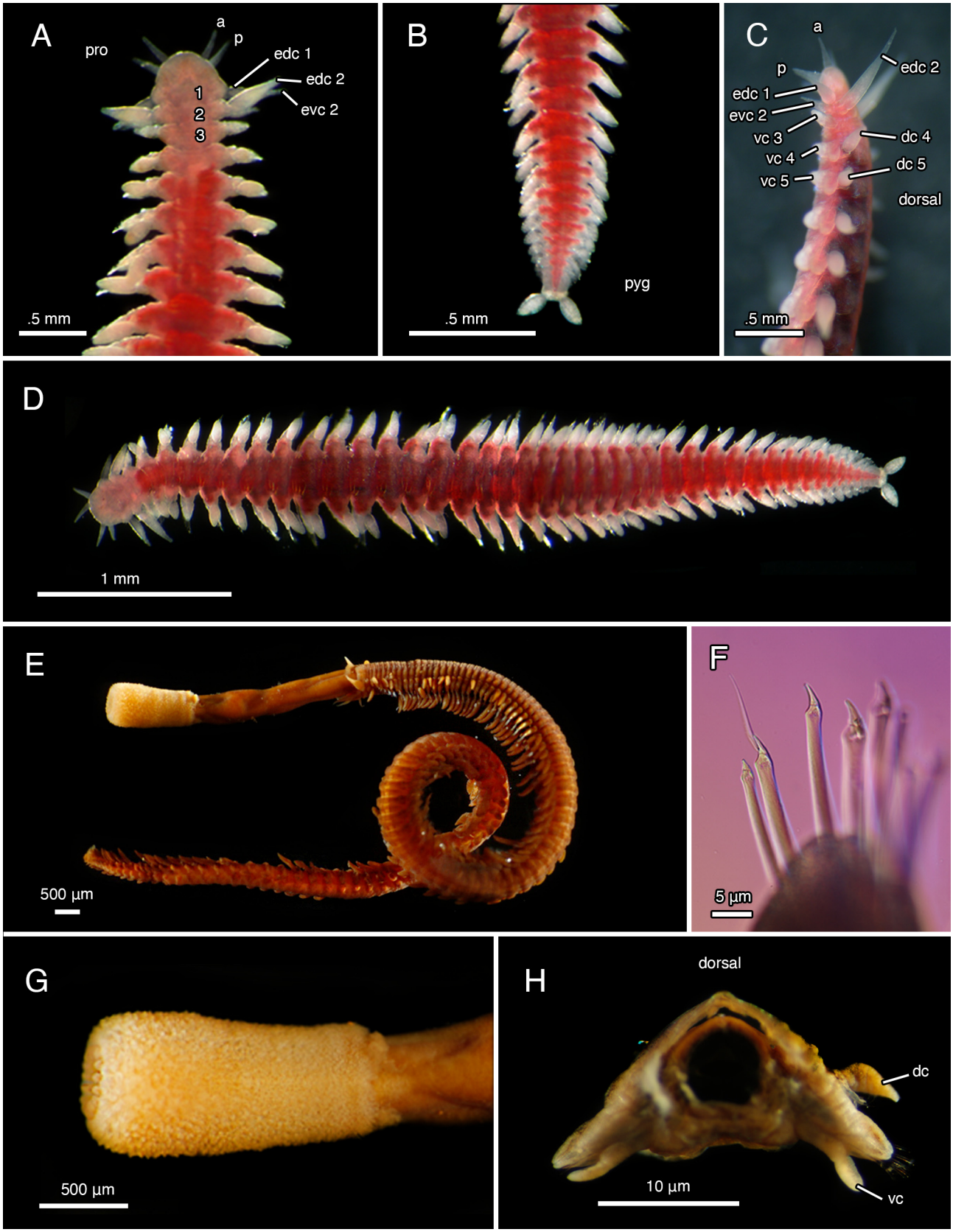

FIGURE 8. Light microscopy (LM) images of *Galapagomystides aristata* from the East Pacific Rise. A—dorsal view of anterior, live (SAMA E8989). B—pygidium, live (SAMA E8989). C—lateral view of anterior, live (SAMA E8991). D—dorsal view of whole body, live (SAMA E8989). E—everted proboscis (SAMA E9002). F—compound chaetae (SAMA E8999). G—proboscis (SAMA E9002). H—parapodia (SAMA E8999). Abbreviations: a, antennae; dc, dorsal cirri; edc, elongated dorsal cirri; evc, elongated ventral cirri; vc, ventral cirri; p, palps; pro, prostomium; pyg, pygidium.

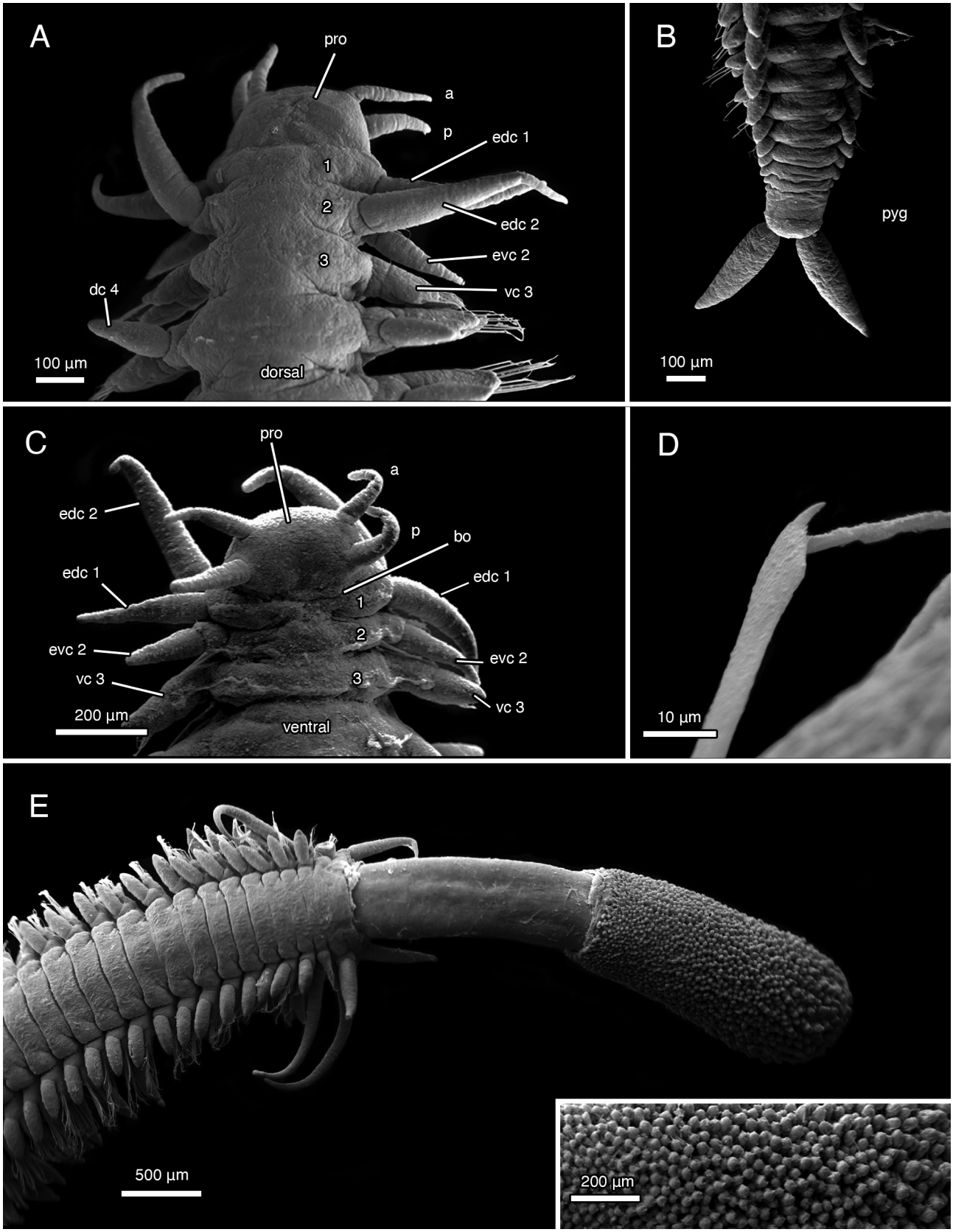

FIGURE 9. Scanning electron microscopy (SEM) images of *Galapagomystides aristata* from the East Pacific Rise. A—dorsal view of anterior (SAMA E9001). B—pygidium (SAMA E9001). C—ventral view of anterior (SAMA E9001). D—zoomed-in compound chaetae joint (SAMA E9002). E—everted proboscis, with zoomed-in inlay of papillae (SAMA E9002). Abbreviations: a, antennae; bo, buccal organ; dc, dorsal cirri; edc, elongated dorsal cirri; evc, elongated ventral cirri; vc, ventral cirri; p, palps; pro, prostomium; pyg, pygidium.

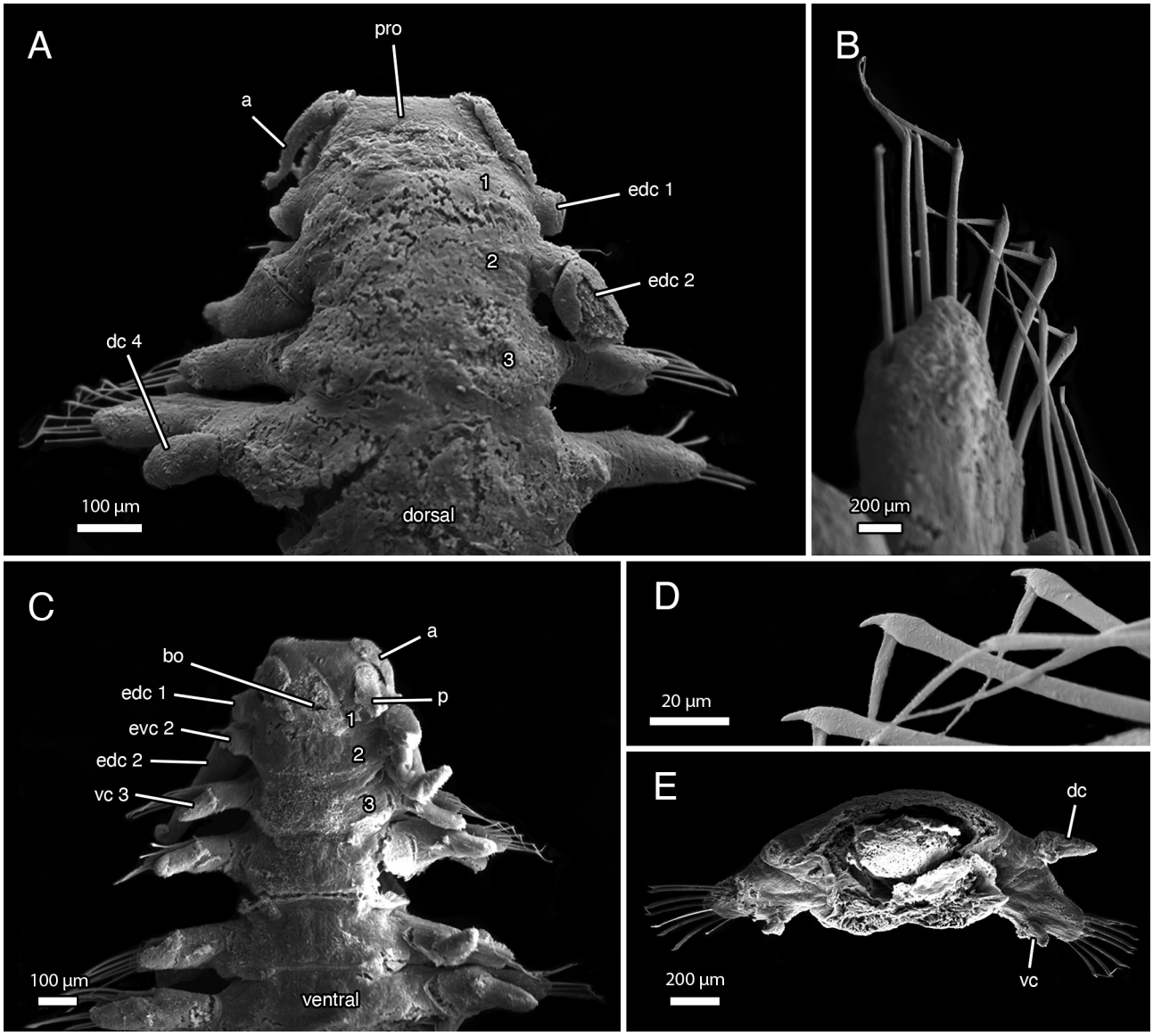

FIGURE 10. Scanning electron microscopy (SEM) images of *Galapagomystides aristata,* paratype voucher (SIO-BIC A13574). A—dorsal view of anterior. B—compound chaetae. C—ventral view of anterior. D—compound chaetae joint. E—parapodia. Abbreviations: a, antennae; bo, buccal organ; dc, dorsal cirri; edc, elongated dorsal cirri; evc, elongated ventral cirri; vc, ventral cirri; p, palps; pro, prostomium; pyg, pygidium.

Galapagomystides verenae (Blake and Hilbig 1990) new combination

Figures 11–14

Bergquist *et al*. (2007: 53, 62), (Blake and Hilbig 1990:xx), Chapman *et al*. (2018: 572, 573), Desbruyères *et al*. (1997: 82), Desbruyères *et al*. 2006: 217), Kelly *et al*. (2007: 6), Lelièvre *et al*. (2017: 2633, 2637-2639), Milligan and Tunnicliffe (1994: 4781), Tsurumi and Tunnicliffe (2003: 617, 625), Tunnicliffe (1992: 340), Tunnicliffe *et al*. (1998: 367).

Material Examined. Paratype: SIO-BIC A13575 (transferred from USNM, used for SEM), Magic Mountain, Explorer Ridge, USA, ~1,810 m depth. Vouchers: SIO-BIC: A7991(A–M)*, Axial Seamount (CASM), Juan de Fuca Ridge, ~1,550 m depth; SIO-BIC: A3263(A–E)*, A8563(A-D)*, Guaymas Basin, Mexico, ~1,650 m depth; SIO-BIC: A1496A*, A1496B*, A1477A*, A1312*, A1331*, A1918*, Mound 12, Costa Rica, 1,000 m depth; SIO-BIC: A1830(A–D)*, A8359*, A8379*, A10044*, Jaco Scar, Costa Rica, ~1,800 m depth; SIO-BIC: A8466*, A8353*, Parrita Seep, Costa Rica, ~1,400–1,800 m depth. For locality details see Table 1. * indicates sequenced specimens.

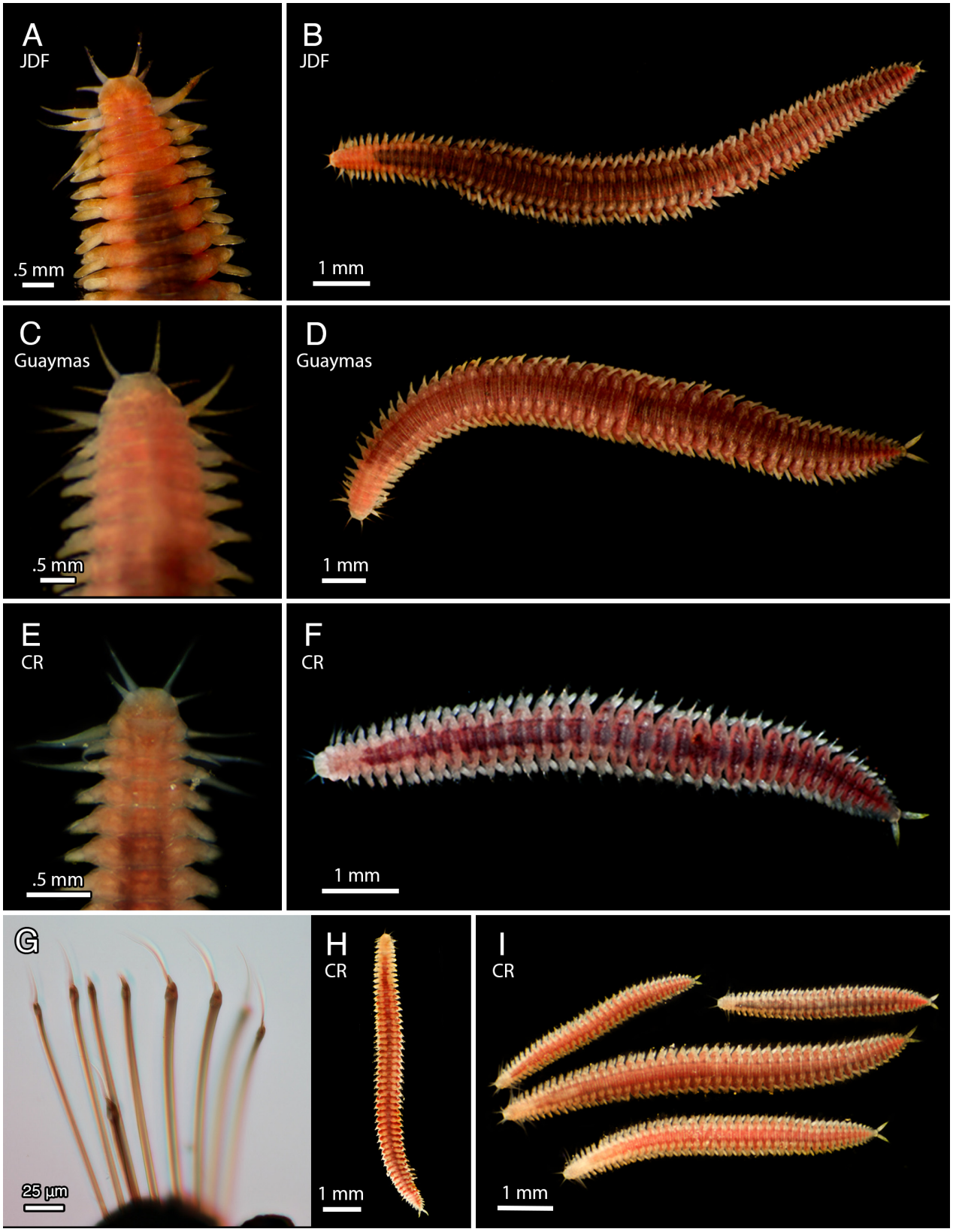

FIGURE 11. Light microscopy (LM) images of live *Galapagomystides verenae* n. comb. from different regions. A—dorsal view of anterior (SIO-BIC A7991, Juan de Fuca Ridge). B—dorsal view of the whole worm (SIO-BIC A7991, Juan de Fuca Ridge). C—dorsal view of anterior (SIO-BIC A3263, Guaymas Basin). D—dorsal view of the whole worm (SIO-BIC A3263, Guaymas Basin). E—dorsal view of anterior (SIO-BIC A10044, Costa Rica). F—dorsal view of whole worm (SIO-BIC A10044, Costa Rica). G—compound chaetae (SIO-BIC A1830, Costa Rica). H—dorsal view of the whole worm (SIO-BIC A8466, Costa Rica). I—dorsal view of whole worms (SIO-BIC A8466, Costa Rica).

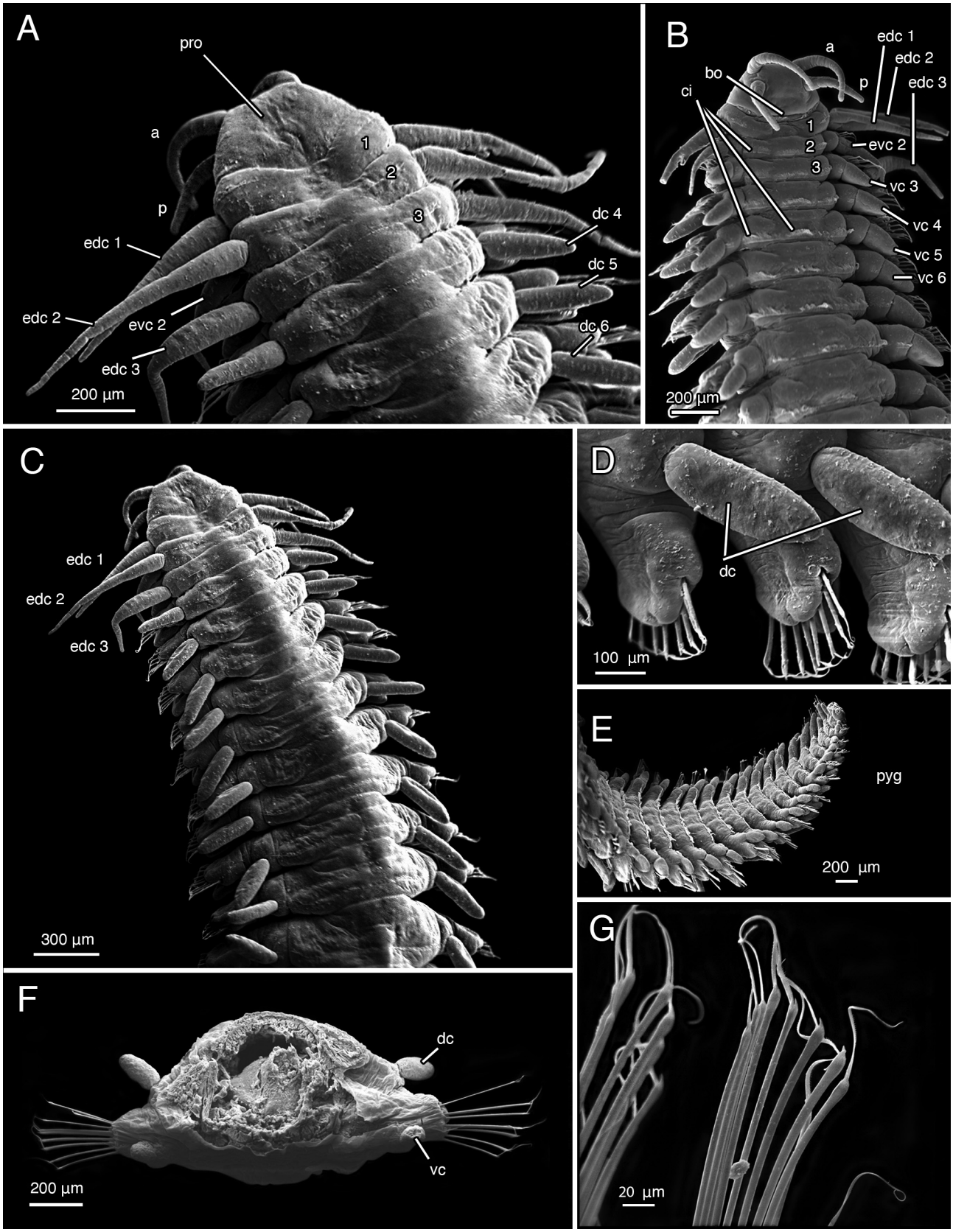

FIGURE 12. Scanning electron microscopy (SEM) of *Galapagomystides verenae* n. comb. (SIO-BIC A7991, Juan de Fuca Ridge). A—dorsal view of anterior. B—ventral view of anterior. C—dorsal view of anterior. D—parapodia, dorsal cirri and chaetae. E—ventral/lateral view of pygidium. F—parapodia. G—compound chaetae. Abbreviations: a, antennae; bo, buccal organ; ci, cilia; dc, dorsal cirri; edc, elongated dorsal cirri; evc, elongated ventral cirri; vc, ventral cirri; p, palps; pro, prostomium; pyg, pygidium.

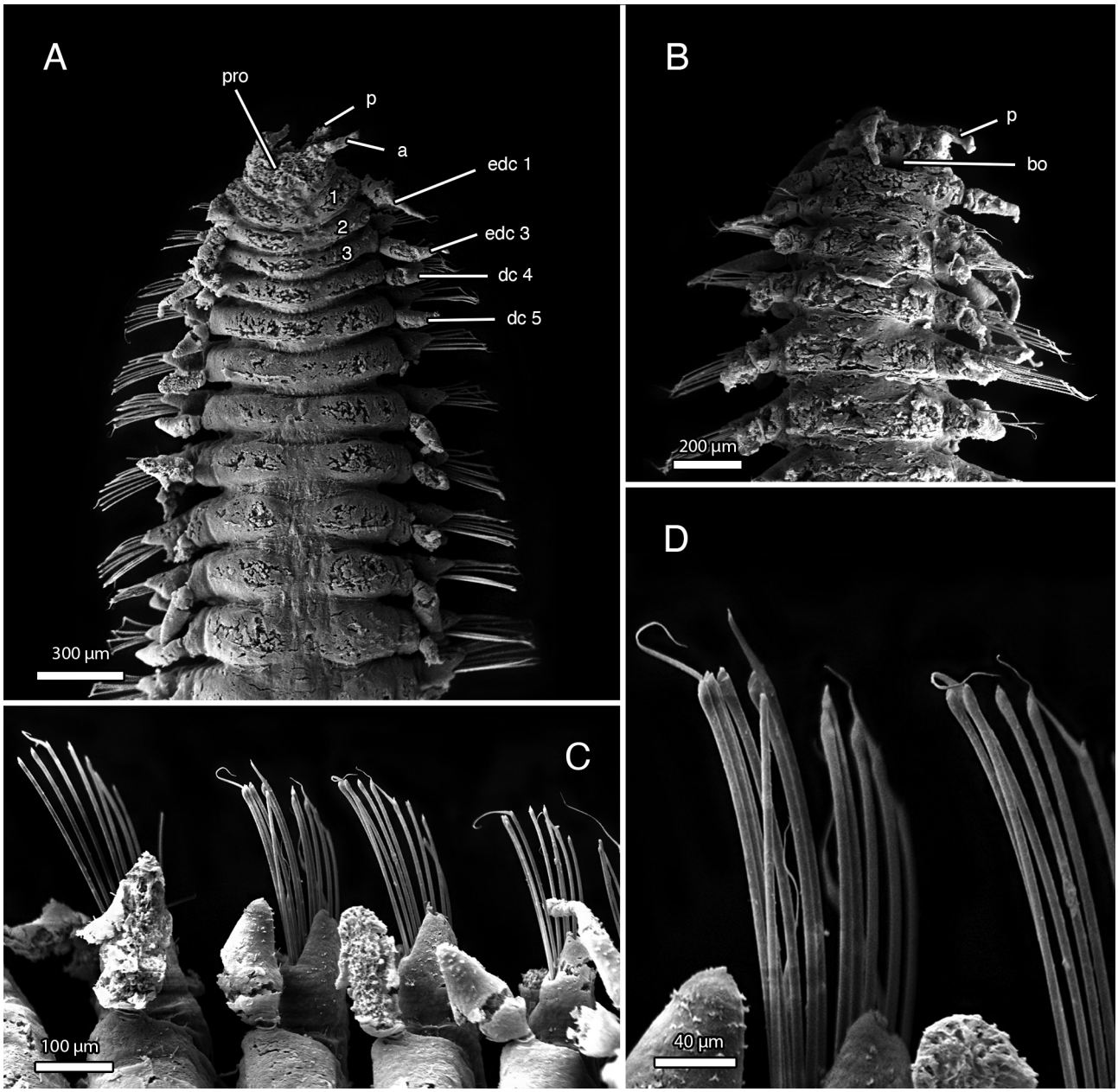

FIGURE 13. Scanning electron microscopy (SEM) of *Galapagomystides verenae* n. comb., paratype from the type locality (SIO-BIC A13575). A—dorsal view of anterior. B—ventral view of anterior. C—lateral view of parapodia and chaetae fascicles. D—detail of compound chaetae. Abbreviations: a, antennae; bo, buccal organ; dc, dorsal cirri; edc, elongated dorsal cirri; p, palps; pro, prostomium.

Diagnosis. First segment not fused to prostomium. Trapezoidal prostomium that is dorsally "V" shaped posteriorly. Elongated dorsal cirri on segments 1, 2 and 3. Elongated ventral cirri on segment 2.

Description. Up to 25 mm long, 1 mm wide at segment 10 for ~60 segments. Body red longitudinal stripe in life, semi-translucent white/pink at parapodial lobes. Dorsal and ventral cirri, elongated cirri, pygidial cirri, prostomium and pygidium also white/pink (Figs 11, 14). Trapezoidal prostomium, "V" shaped posteriorly (Figs 12A, C, 13A); nuchal organs not visible. Anterior dorsal edge of prostomium with paired cylindrical antennae ~0.25 mm long (Fig. 12B). Paired palps ventral to antennae, similar in shape, slightly shorter (Fig. 12B). Segment one distinct from prostomium, following segments also clearly demarcated (Fig. 12A, C). Pair of elongated dorsal cirri [tentacular cirri] on each of segments 1 (~0.4 mm long), 2 (~0.5 mm long), 3 (~0.4 mm long) (Fig. 12A, C). All elongated dorsal cirri cirriform, tapering distally. Pair of elongated ventral cirri on segment 2 (~0.2 mm long) (Fig. 11B). Bulbous, rounded dorsal cirri (~0.15 mm long) begin on segment 4 continuing posteriorly (Fig. 12A, D).

Dorsal cirri larger than ventral cirri. Conical, tapering ventral cirri (~0.1 mm long) begin on segment 3 continuing posteriorly (Fig. 12B). Ventral cilia bands present (Fig. 12B). Parapodia uniramous, notopodial chaetae absent; neuropodium with central fascicle containing ~5–8 compound chaetae; one simple emergent acicula (Figs 11G, 12F, G). Compound chaetal shaft cylindrical; thin, flattened pointed curled blade extended from curved joint (Figs 11G, 12F, G). Pygidium with one pair of cirriform pygidial cirri tapering distally (~0.2 mm long) (Fig. 11B, D, F).

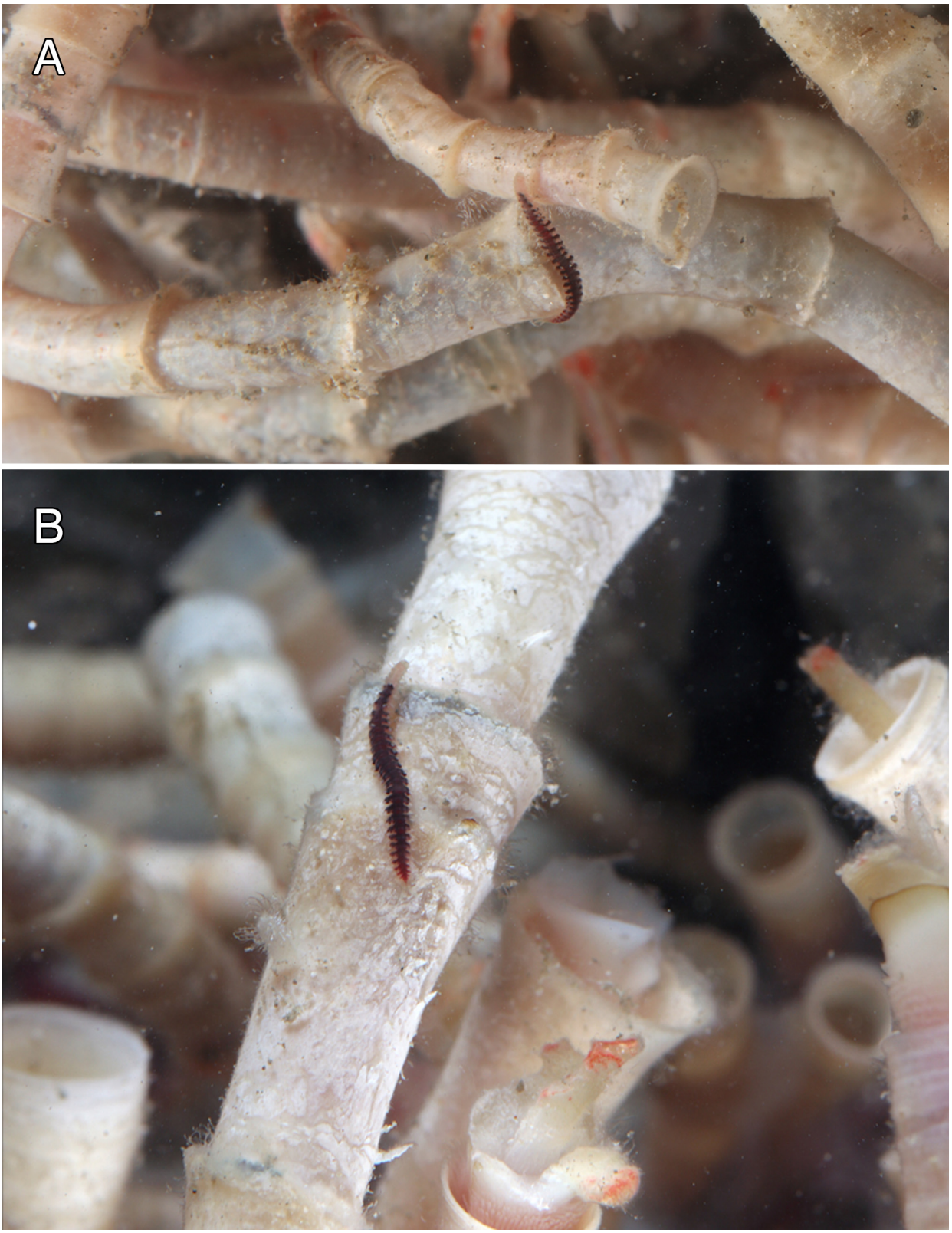

FIGURE 14. A & B—in situ dorsal-view images of *Galapagomystides verenae* n. comb. associated with juvenile *Escarpia spicata* tubes at Parrita Seep off Costa Rica.

Variation. Material examined in this study largely matches the original description (Blake and Hilbig 1990). The largest SIO-BIC specimen was 25 mm long (SIO-BIC A7991, Axial seamount vents, JDF), slightly shorter than the original description at 27 mm long (Blake and Hilbig 1990). *Galapagomystides verenae* n. comb. specimens collected from Costa Rica and Guaymas had the similar lengths reported from the type locality.

Remarks. Blake and Hilbig (1990) argued that *Galapagomystides verenae* n. comb. was a member of *Protomystides* owing to the absence of fusion between the prostomium and segment 1, the position and orientation of the elongated dorsal and ventral cirri, and its lobed pygidial cirri. While these observations are correct, the phylogenetic position based on DNA means that it should be moved to *Galapagomystides.* Observations of living *G. verenae* n. comb. are reported for the first time and its red color is like other species of *Galapagomystides* (Figs 11, 14). Also, images of *Galapagomystides verenae* n. comb., on top of juvenile *Escarpia spicata* (Vestimentifera) tubes from Costa Rica seeps supports the hypothesis that these worms may be blood feeders (Fig. 14).

Unique features for *G. verenae* n. comb. include a trapezoidal prostomium that is dorsally "V" shaped posteriorly (Figs 12A and 13A), chaetal blade length and curl (Figs 12G and 13D), and the conical shape of ventral cirri (Figs 12B and 13C). The total range of *G. verenae* spans from ~9°N, to ~46°N, from the seeps of Guaymas Basin and Costa Rica margin to the hydrothermal vents of the Juan de Fuca Ridge. *Galapagomystides verenae* n. comb. is unique among *Galapagomystides* for being present at both seeps and vents and appears to have occupied vents from a seep ancestry (Fig. 6). *Galapagomystides verenae* n. comb. is morphologically most like *G. patricki* n. sp., with both species showing no fusion of anterior segments with the prostomium. However, in the phylogenetic analyses, *G. verenae* n. comb. was found to be the sister taxon to *G. kathyae* n. sp. (Fig. 2).

Galapagomystides bobpearsoni n. sp.

Figures 15, 16

Diagnosis. First segment fused dorsally to prostomium. Elongated dorsal cirri on segments 1, 2 and 3. The elongated dorsal cirri on segments 2 and 3 are the longest of all *Galapagomystides* species. Elongated ventral cirri on segment 2.

Material Examined. Holotype: SIO-BIC A4588* (prepared for SEM), Tow Cam vent, Lau Back-arc Basin, Tonga, ~2720 m depth, May 19, 2005, ROV Jason II. [Genbank COI = MZ711262] Paratype: SIO-BIC A4590 collected from Tui Malila, Lau Back-arc Basin, Tonga, ~1890 m depth. For locality details see Table 1. * indicates sequenced specimen.

Description. Holotype length unknown (incomplete- missing posterior end used for DNA sequencing). Body width 0.8 mm at segment 10 (Figs 15A, 16C). Body light pink in life (Fig. 15C). Body brown/orange with numerous dark pigmentation speckles in preserved (formalin/ethanol) state (Fig. 15A, B). Prostomium slightly wider than long; nuchal organs not visible (Fig. 16A, D). Anterior dorsal edge of prostomium with paired cylindrical antennae ~0.25 mm long (Fig. 16A). Paired palps ventral to antennae, similar in shape and length to antennae (Fig. 16D). Segment 1 fused to prostomium, following segments clearly demarcated (Fig. 16A). Pair of elongated dorsal cirri [tentacular cirri] on each of segments 1 (~0.3 mm long), 2 (~0.42 mm long) and 3 (~0.44 mm long) (Fig. 16A, D). All elongated dorsal cirri cirriform, tapering distally. Ventral cirri absent from segment 1 (Fig. 16D). Pair of elongated ventral cirri on segment 2 ~0.3 mm long (Fig. 16D). Bulbous, rounded dorsal cirri ~0.1 mm long begin on segment 3 continuing posteriorly (Fig. 16C). Cylindrical, tapering ventral cirri ~0.1 mm long begin on segment 3 continuing posteriorly (Fig. 16D). Parapodia uniramous, notopodial chaetae absent; neuropodium with central fascicle containing ~5–9 compound chaetae; one simple emergent acicula (Figs 15D, E, F, G, 16E, F). Compound chaetal shaft cylindrical; thin, flattened pointed blade extended from curved joint (Fig. 15E).

Variation. Only two specimens were collected. The paratype matches the holotype, but is also complete with a pygidium, which has a pair of small lobed cirri ~0.2 mm long, rounded distally.

Remarks. *Galapagomystides bobpearsoni* n. sp. is morphologically like *G. aristata* and *G. kathyae* n. sp. in having segment 1 dorsally fused to the prostomium. However, in the phylogenetic analyses *G. bobpearsoni* n. sp. was found to be the sister group to a clade comprising *G. aristata*, *G. kathyae* n. sp. and *G. verenae* n. comb. (Fig. 2) *Galapagomystides bobpearsoni* n. sp. is restricted to Lau Back-arc Basin between 1890–2720 m depth. An obvious morphological feature distinguishing *G. bobpearsoni* n. sp. is the very long cirriform elongated dorsal cirri originating from the first three segments, the longest projecting from segments two and three. The chaetal blades of *G. bobpearsoni* n. sp. are also notable for being the longest of all *Galapagomystides* species.

Etymology. *Galapagomystides bobpearsoni* n. sp. is named after the lead author's father, Bob Pearson, for his invaluable love and support, and who inspired the lead author's passion and curiosity for the ocean.

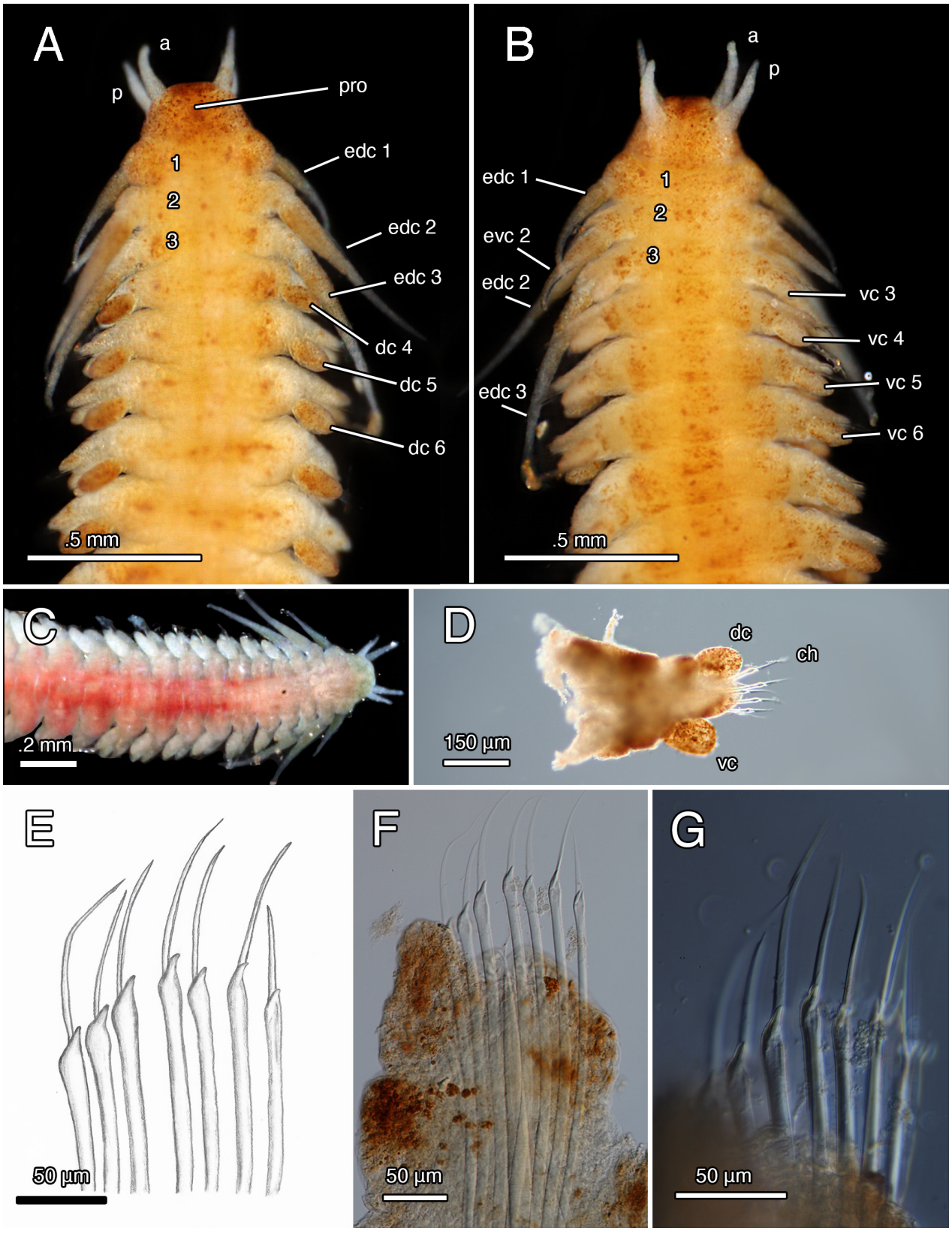

FIGURE 15. Light microscopy (LM) images of *Galapagomystides bobpearsoni* n. sp. holotype (SIO-BIC A4588). A—dorsal view. B—ventral view. C—dorsal view of anterior, live. D—parapodia. E—drawing of compound chaetae. F—compound chaetae. G—compound chaetae. Abbreviations: a, antennae; dc, dorsal cirri; edc, elongated dorsal cirri; evc, elongated ventral cirri; vc, ventral cirri; p, palps; pro, prostomium.

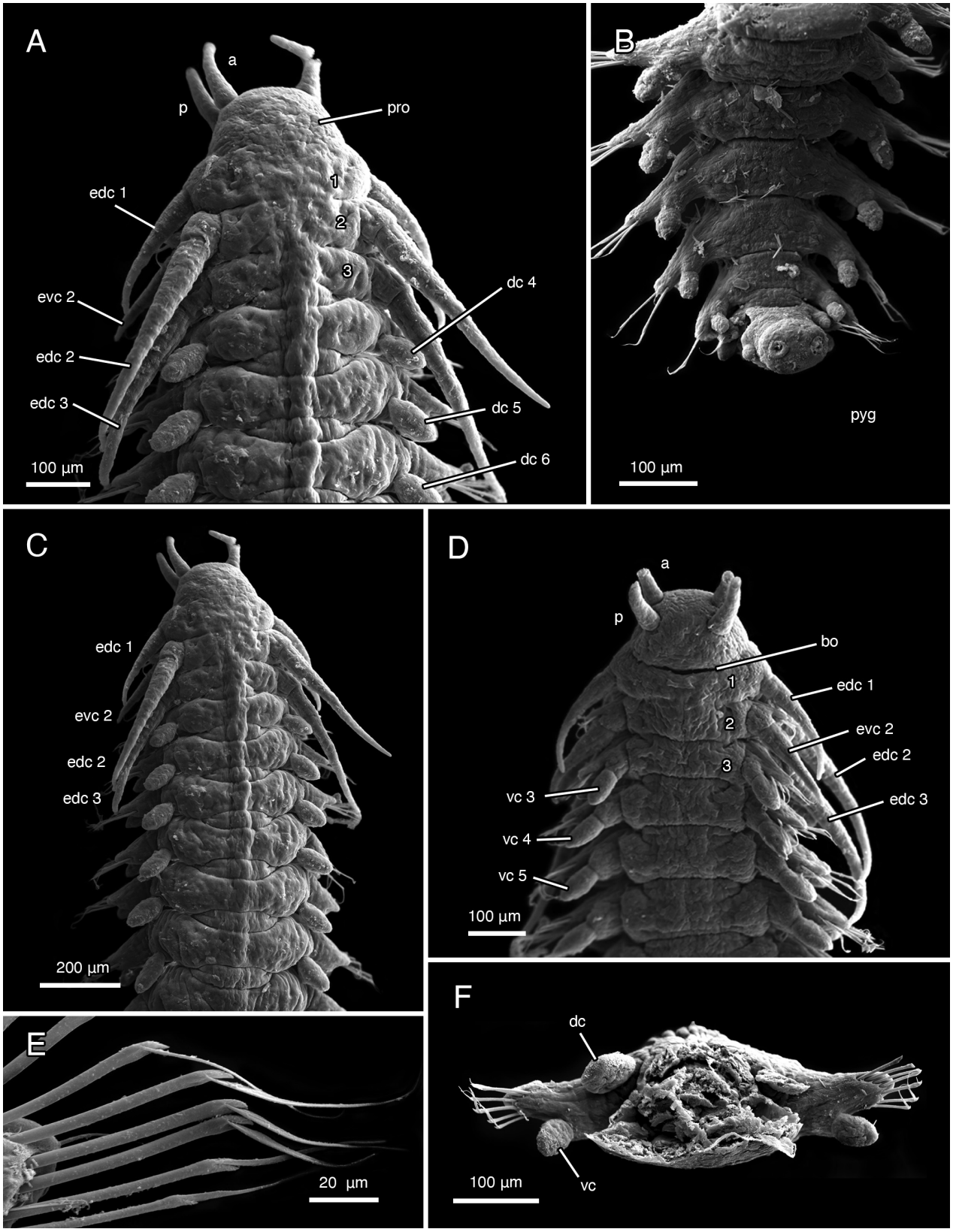

FIGURE 16. Scanning electron microscopy (SEM) of *Galapagomystides bobpearsoni* n. sp. A—close-up dorsal view of anterior and prostomium, holotype (SIO-BIC A4588). B—ventral view of pygidium (pygidial cirri broke off, two scars seen at distal end), paratype (SIO-BIC A4590). C—dorsal view of anterior, holotype (SIO-BIC A4588). D—ventral view of anterior (tips of antennae and palps broken off), holotype (SIO-BIC A4588). E—compound chaetae, holotype (SIO-BIC A4588). F—parapodia, holotype (SIO-BIC A4588). Abbreviations: a, antennae; bo, buccal organ; dc, dorsal cirri; edc, elongated dorsal cirri; evc, elongated ventral cirri; vc, ventral cirri; p, palps; pro, prostomium; pyg, pygidium.

***Galapagomystides kathyae* n. sp.**
Figures 17, 18

Diagnosis. First segment fused dorsally to prostomium. Wider prostomium. Elongated dorsal cirri on segments 1, 2 and 3. Elongated ventral cirri on segment 2.

Material Examined. Holotype: SIO-BIC A13418* (prepared for SEM), White Lady vent, North Fiji Basin, Fiji, 16.9905° S 173.9147° E, ~1990 m depth, June 1, 2005, ROV Jason II. [GenBank COI= MZ711261] **Paratypes:** SIO-BIC A13422, A13423, A13424, A4651, A4645, White Lady vent, North Fiji Basin, Fiji, ~1990 m depth; A4587, Tow Cam, Lau Back-arc Basin, Tonga, ~2720 m depth. For locality details see Table 1. * indicates sequenced specimens.

Description. Holotype body length 14 mm long, 1 mm wide at segment 10 for ~65 segments. Body deep pink in life (Fig. 17C). Body brown/orange with numerous dark pigmentation speckles in preserved (formalin/ethanol) state (Fig. 17A, B, D). Lobe-like prostomium; nuchal organs not visible (Fig. 18A). Anterior dorsal edge of prostomium with paired cylindrical antennae ~0.2 mm long (Fig. 18A, D). Paired palps ventral to antennae, similar in shape and length to antennae (Fig. 18D). Segment one dorsally fused to prostomium, following segments clearly demarcated (Fig. 18A). Pair of elongated dorsal cirri [tentacular cirri] on each of segments 1 (~0.25 mm long), 2 (~0.25 mm long) and 3 (~0.2 mm long) (Fig. 18A). All elongated dorsal cirri cirriform, tapering distally. Pair of elongated ventral cirri on segment 2 ~0.15 mm long (Fig. 18D). Bulbous, rounded dorsal cirri ~0.08 mm long begin on segment 4 continuing posteriorly (Fig. 18A, C). Conical, tapering ventral cirri ~0.1 mm long begin on segment 3 continuing posteriorly (Fig. 18D). Ventral cilia bands present (Fig. 18D). Parapodia uniramous, notopodial chaetae absent; neuropodium with central fascicle containing ~5–8 compound chaetae; one simple emergent acicula (Figs 17E, F, G, 18F). Compound chaetal shaft cylindrical; thin, flattened pointed blade extended from curved joint (Fig. 17E). Pygidium with one pair of small lobed cirriform pygidial cirri ~0.1 mm long rounded distally (Fig. 18B).

Variation. Paratypes largely match the holotype. The paratype SIO-BIC A4651 of *G. kathyae* n. sp. is a juvenile (Fig. 17D), has less segments and is smaller than the holotype. This specimen was not sequenced but the morphology matches the holotype.

Remarks. *Galapagomystides kathyae* n. sp. is morphologically most like *G. aristata* and *G. bobpearsoni* n. sp. in having segment 1 dorsally fused to the prostomium. However, in the phylogenetic analyses, *G. kathyae* n. sp. was the sister group to *G. verenae* (Fig. 2). *Galapagomystides kathyae* n. sp. was found at both the North Fiji Basin and Lau Back-arc Basin, separated by 1110 km. The single specimen collected from the Lau Back-arc Basin does not have a DNA sequence but was morphologically like the holotype. The distinguishing morphological characteristics of *G. kathyae* n. sp. are a wide prostomium and elongated dorsal cirri originating from the second segment having a marked 90° angle distal to the body. The chaetal blades of *G. kathyae* n. sp. are thin and appear delicate, originating from a pointed joint.

Etymology. *Galapagomystides kathyae* n. sp. is named after the lead author's mother, Kathy Reimer-Pearson, for her invaluable love and support, and who sparked the lead-author's interest and enthrallment in invertebrates.

***Galapagomystides patricki* n. sp.**
Figures 19, 20

Diagnosis. First segment not fused to prostomium. Elongated dorsal cirri on segments 1 and 2. No elongated ventral cirri.

Material Examined. Holotype: SIO-BIC A13419* (prepared for SEM), Parrita Seep, Costa Rica; 9.0303° N 84.623° W, ~1415 m depth, March 1, 2009, HOV Alvin. [Genbank COI= MZ711314] **Paratypes:** SIO-BIC: A13425, A13426, A13427, A13420*, A13421*, Parrita Seep, Costa Rica ~1400 m depth; SIO-BIC: A9964*, A9875*, A9877*, A9961*, A9934, Parrita Seep, Costa Rica ~850 m depth; MZUCR 1510-01*, Jacó Scar, Costa Rica, ~1770 m depth; SIO-BIC: A1424, ~20 km away Parrita Seep, ~805 m depth. For locality details see Table 1. * indicates sequenced specimens.

Description. Holotype body length 16 mm, 1mm wide at segment 10 for ~70 segments. Body red or white with red gut in life (Fig. 19A). Body brown/orange with numerous dark pigmentation speckles in preserved (formalin/ethanol) state (Fig. 19C, D). Lobe-like prostomium; nuchal organs not visible (Fig. 20A). Anterior dorsal edge of

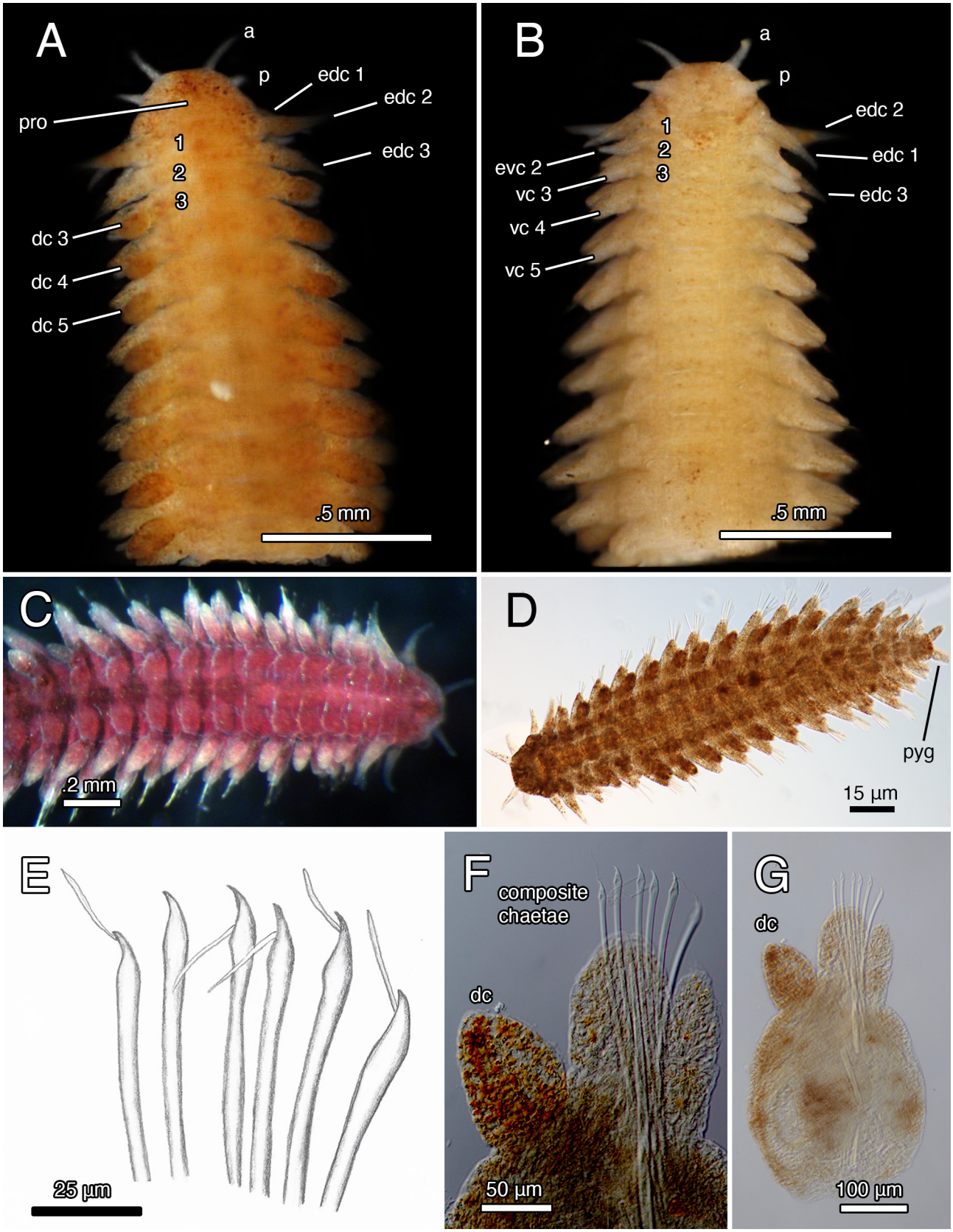

FIGURE 17. Light microscopy (LM) images of *Galapagomystides kathyae* n. sp. A—dorsal view, holotype (SIO-BIC A13418). B—ventral view of holotype, holotype (SIO-BIC A13418). C—live dorsal view, holotype (SIO-BIC A13418). D—whole body, paratype (SIO-BIC A4651). E—drawing of compound chaetae, holotype (SIO-BIC A13418). F—dorsal cirri, holotype (SIO-BIC A13418). G—parapodia, holotype (SIO-BIC A13418). Abbreviations: a, antennae; dc, dorsal cirri; edc, elongated dorsal cirri; evc, elongated ventral cirri; vc, ventral cirri; p, palps; pro, prostomium; pyg, pygidium.

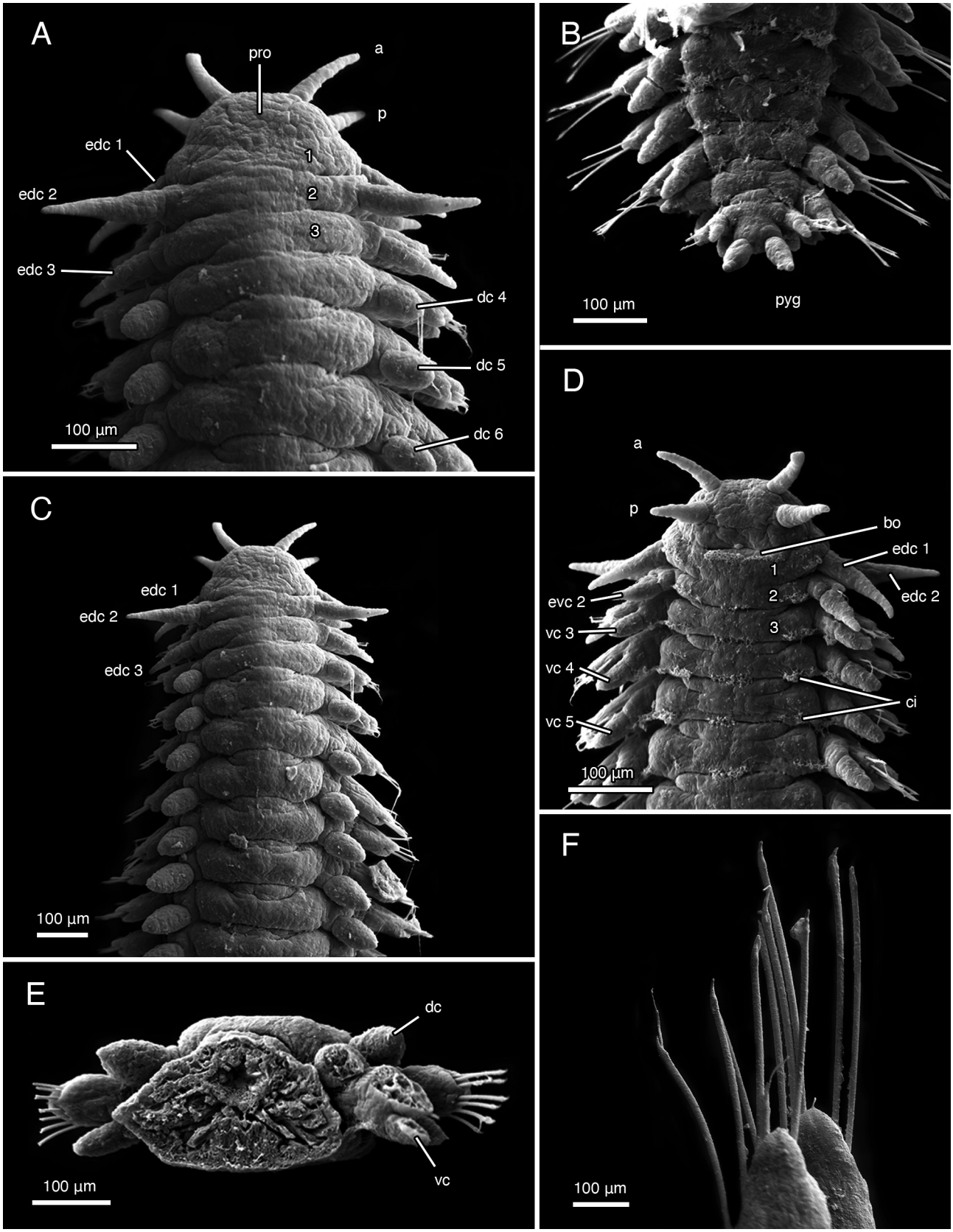

FIGURE 18. Scanning electron microscopy (SEM) of *Galapagomystides kathyae* n. sp. holotype (SIO-BIC A13418). A—close-up dorsal view of anterior and prostomium. B—ventral view of pygidium with pygidial cirri. C—dorsal view of anterior. D—ventral view of anterior. E—parapodia. F—compound chaetae. Abbreviations: a, antennae; bo, buccal organ; ci, cilia; dc, dorsal cirri; edc, elongated dorsal cirri; evc, elongated ventral cirri; vc, ventral cirri; p, palps; pro, prostomium; pyg, pygidium.

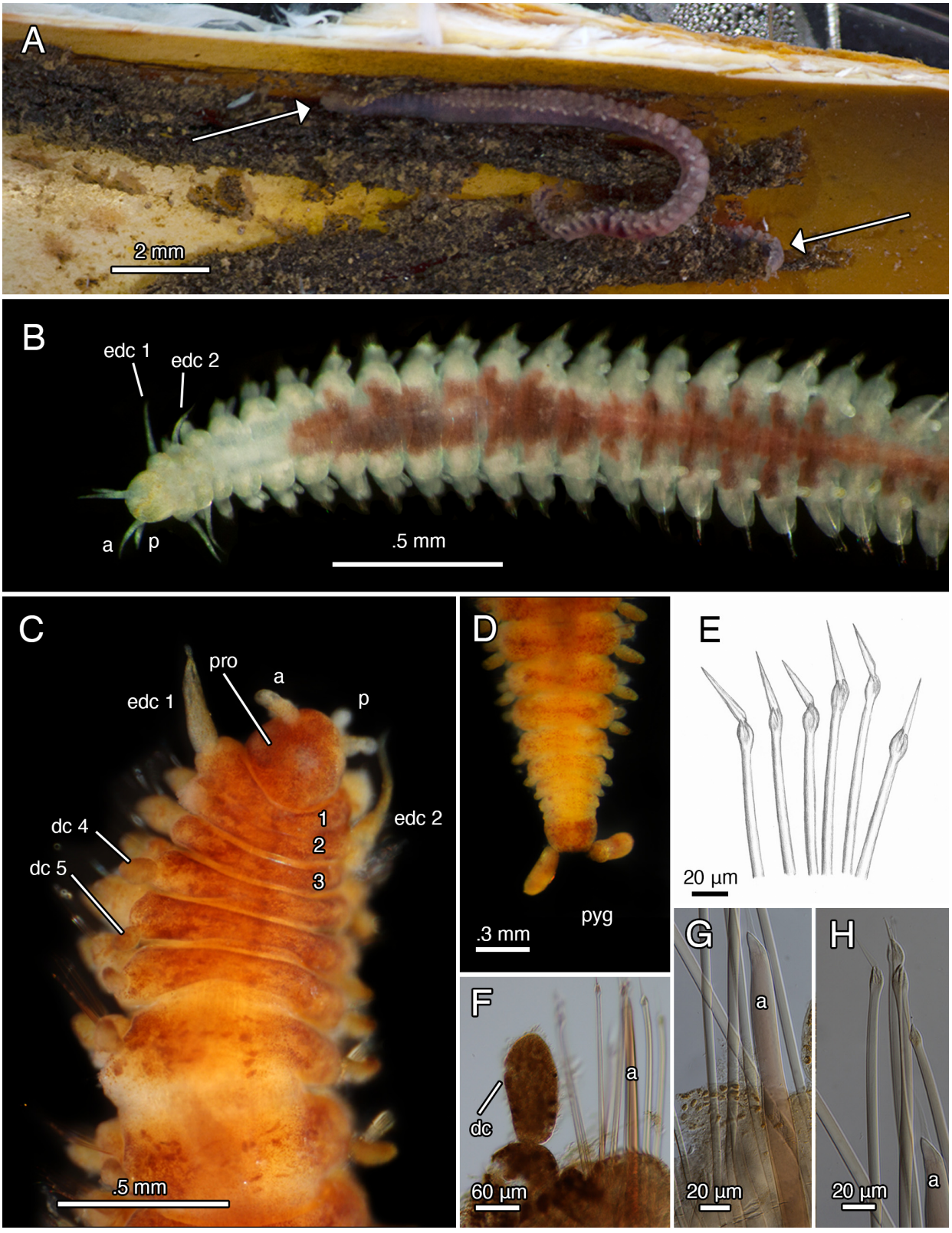

FIGURE 19. Light microscopy (LM) images of *Galapagomystides patricki* n. sp. A—*in situ Galapagomystides* inside Vestimentiferan tube, Alvin Dive 4508, Mound Quepos, Parrita Seep, Costa Rica, paratype (SIO-BIC A13420; A13420). B—dorsal view of anterior, paratype (SIO-BIC A1424). C—dorsal view of anterior and prostomium, holotype (SIO-BIC A13419). D—dorsal view of pygidium with pygidial cirri, holotype (SIO-BIC A13419). E—drawing of compound chaetae, holotype (SIO-BIC A13419). F—dorsal cirri, holotype (SIO-BIC A13419). G—aciculum, holotype (SIO-BIC A13419). H—compound cirri, holotype (SIO-BIC A13419). Abbreviations: a, antennae; a, aciculum; dc, dorsal cirri; edc, elongated dorsal cirri; p, palps; pro, prostomium; pyg, pygidium.

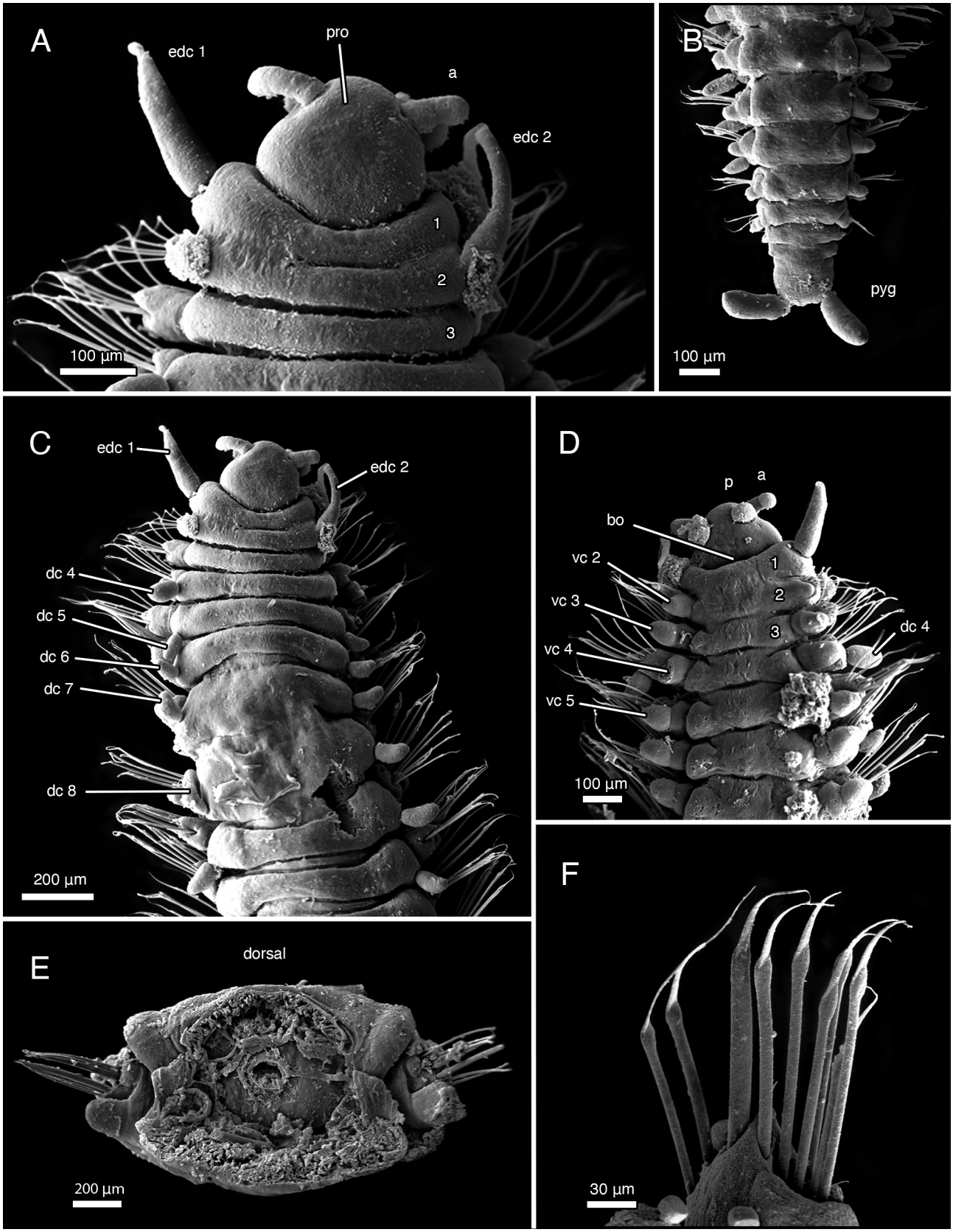

FIGURE 20. Scanning electron microscopy (SEM) of *Galapagomystides patricki* n. sp. holotype (SIO-BIC A13419). A—close-up dorsal view of anterior and prostomium. B—dorsal view of pygidium with pygidial cirri. C—dorsal view of anterior. D—ventral view of anterior. E—parapodia. F—compound chaetae. Abbreviations: a, antennae; bo, buccal organ; dc, dorsal cirri; edc, elongated dorsal cirri; vc, ventral cirri; p, palps; pro, prostomium; pyg, pygidium.

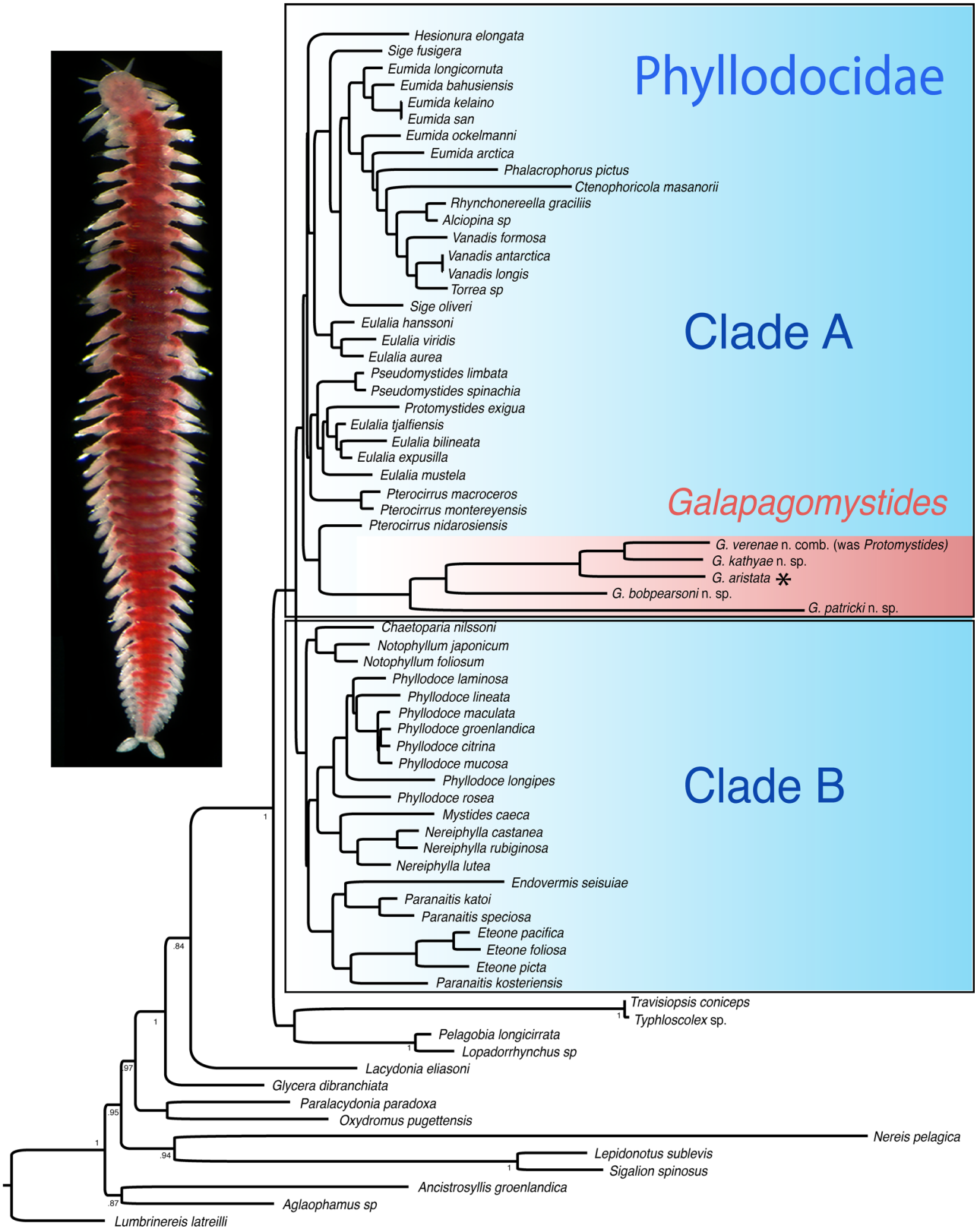

FIGURE 21. Maximum Likelihood (ML) tree rendered from the concatenation of genes COI, 18S, 28S and 16S including outgroups (rooted with *Lumbrineris latreilli*), that were not shown in Figure 2. '*' indicates type species of *Galapagomystides*. Support values are not shown for the parts of the topology seen in Figure 2. Numbers on nodes represent ML bootstrap values (above node) and Bayesian posterior probabilities (below node). Values below 50% for ML and 0.70 for posterior probabilities are not shown.

prostomium with paired cylindrical antennae (~0.25 mm long) (Fig. 20A). Paired palps ventral to antennae, similar in shape and length to antennae (Fig. 20A, D). Segment one not fused to prostomium, distinct dorsally and ventrally, following segments clearly demarcated (Fig. 20A, C). Pair of elongated dorsal cirri [tentacular cirri] on each of segments 1 (~0.4 mm long), 2 (~0.35 mm long) (Fig. 20A). All elongated dorsal cirri cirriform, tapering distally (Fig. 20A). Dorsal elongated cirri on segment one, right side and dorsal elongated cirri on segment two, left side were broken off the holotype. No elongated ventral cirri (Fig. 20D). Segment 3 lacking dorsal cirri (Figs 19B, C, 20A). Bulbous, rounded dorsal cirri (~0.1 mm long) begin on segment 4 continuing posteriorly (Fig. 20C). Ventral cirri absent on segment 1 (Fig. 20D). Bulbous ventral cirri (~0.1 mm long) (Fig. 20D). Chaetae begin on segment 2 continuing posteriorly (Fig. 20A). Parapodia uniramous, notopodial chaetae absent; neuropodium with central fascicle containing ~6–10 compound chaetae; one simple emergent acicula (Figs 19E, F, G, H, 20F). Compound chaetal shaft cylindrical; thin, flattened triangular short blade extending from rounded joint (Figs 19E, 20F). Pygidium with one pair of lobed pygidial cirri (~0.15 mm long) rounded distally (Fig. 20B).

Variation. Most *G. patricki* n. sp. type material specimens were within $^{+}$/- 1 to 3 mm from the holotype in overall length, though one juvenile was ~10 mm smaller than the holotype. The specimens ranged from ~40 segments to ~70 segments. In life, the paratypes of *G. patricki* n. sp. had a body that was semi-translucent white/pink at parapodial lobes, dorsal and ventral cirri, prostomium and pygidium; red in the gut region center with a yellow patch on prostomium, elongated cirri and pygidial cirri (Fig. 19B).

Remarks. Most *G. patricki* n. sp. samples were collected from Parrita Seep, Costa Rica (1400 m), except for one specimen collected from the deeper Jacó Scar, Costa Rica (1800 m). A single sample, A1424, was collected from a multicore that was deployed offsite in the vicinity of the seep. Some *G. patricki* n. sp. specimens were found in sediment tubes inside empty vestimentiferan tubes. Morphologically, *G. patricki* n. sp. is most like *G. verenae* new comb. as both species show no fusion of anterior segments with the prostomium. However, in the phylogenetic analyses, *G. patricki* n. sp. was the sister group to the rest of the genus (Fig. 2). *Galapagomystides patricki* n. sp. lacks dorsal cirri on segment three (all other species have either elongated or regular dorsal cirri on segment three). The chaetae of *G. patricki* n. sp. had the shortest blades compared to other species and are also triangular (while the blades in other species are falcate).

Etymology: *Galapagomystides patricki* n. sp. is named after Patrick Shaughnessy, whose love and support during this project was instrumental to the lead author's success.

Discussion

This is the first study examining the phylogeny, biogeography, and diversity of *Galapagomystides*. By incorporating the new data with those from previous molecular phylogenies of Phyllodocidae (Eklöf *et al*. 2007; San Martín *et al.* 2021) it was possible to assess Pleijel's (1991) hypothesis as to the placement of *Galapagomystides*. Pleijel (1991) proposed that *Galapagomystides* formed the sister group to a clade comprising *Eteone, Hypereteone* and *Mysta.* These taxa along with others such as *Eulalia, Eumida, Protomystides, Pseudomystides, Pterocirrus*, and *Sige* formed the subfamily Eteoninae. The remaining Phyllodocidae were placed in Phyllodocinae (*Chaetoparia*, *Paranaitis* and *Phyllodoce*), and Notophyllinae (*Notophyllum*, *Nereiphylla*). Previously, in his original description of *Galapagomystides aristata*, Blake (1985) suggested that it was closely related to *Mystides*. Our results of the four concatenated molecular markers shows that Pleijel's (1991) tree topology and classification are not supported, with the type species of each subfamily all placed in clade B (Fig. 2). *Galapagomystides* was recovered as the poorly supported sister group to *Pterocirrus nidarosiensis* and is part of clade A, quite distant from *Eteone*. *Mystides* was also found as part of clade A and distant from *Galapagomystides* in clade B. In addition, the morphological similarities for grouping *Galapagomystides* as proposed by Blake (1985) and Pleijel (1991) do not seem to be supported. However, clades A and B were both poorly supported (Fig. 2) and more data are needed to resolve the phylogeny of Phyllodocidae and allow for a taxonomic revision of the group. The long branch shown by the *Galapagomystides* clade may also indicate that its position shown in Figure 2 may not be accurate. As well as documenting three new species, the results show that another vent-dwelling member of Phyllodocidae, *Protomystides verenae*, should be transferred to *Galapagomystides*.

The biogeographical analysis (Fig. 7) indicates that there are two near sympatric species of *Galapagomystides* at western Pacific vents, and three species in the eastern Pacific, two of which are sympatric at Costa Rican seeps.

The western Pacific species, *G. bobpearsoni* n. sp. and *G. kathyae* n. sp., are not each other's closest relatives, suggesting they independently colonized these sites. Also, *G. verenae* n. comb. and *G. patricki* n. sp. were found in proximity off Costa Rica at Parrita Seep and are not closely related. This phenomenon has been observed in other annelid taxa including *Amphisamytha* (Stiller *et al.* 2013), *Archinome* (Borda *et al*. 2013) and *Parougia* (Yen and Rouse, 2020). *Galapagomystides verenae* has a very wide distribution at both vents and seeps and may have colonised the Costa Rican and Guaymas Basin seeps, as it appears to have a vent ancestry (Fig. 6). It is not common to find animal species living at both vents and seeps (Kiel, 2016; Sibuet and Olu, 1998; Wolff, 2005; Watanabe *et al*. 2010; Tunnicliffe *et al*. 1998, 2003; Peek *et al*. 1997). Among annelids, the ampharetid *Amphisamytha fauchaldi* Solís-Weiss & Hernández-Alcántara 1994 live at vents in the Gulf of California and seeps from Oregon to Costa Rica and the amphinomid *Archinome levinae* also lives at vents in the Gulf of California and seeps off Costa Rica (Stiller *et al*. 2013; Borda *et al*. 2013).

Protomystides hatsushimaensis has been recorded from seeps and vents in the northwestern Pacific and associated with Vestimentifera (Kobayashi and Kojima 2017). This species also may prove to be a member of *Galapagomystides* once DNA sequence data is made available. The record of a blood-feeding *'Protomystides'* in the Gulf of Mexico (Becker *et al.* 2013) that has also not been described, let alone sequenced, suggests that further *Galapagomystides* species will be discovered and so the present phylogenetic hypothesis is incomplete.

The type locality of *G. verenae* n. comb. is the Juan de Fuca hydrothermal vent systems along the Cascadia Subduction Zone (CSZ) of the northeastern Pacific Ocean, though from evidence provided here, the species also extends much further south at methane seeps. The type locality of *G. aristata* is at the Galapagos Rift vents and it would appear from this and other studies (Jenkins *et al.* 2002; Govenar *et al.* 2004) that it occurs along the East Pacific Rise. These disjunct vent systems were once connected as part of the Pacific-Farallon Ridge, which was disrupted by subduction under the North America plate nearly 30 million years ago (mya) (Chevaldonné *et al.* 2002). Chevaldonné *et al*. (2002) proposed to use this vicariant event as a way of calibrating molecular clocks and assessed this for several proposed annelid sister species pairs that occurred at the northeastern Pacific vents and the EPR. It was later shown that their proposed sister species pairs were not actually sister taxa and so their molecular clock rate has been questioned (Stiller *et al.* 2013), but the use of the calibration point still has merit. The results shown here suggest that *G. aristata* and *G. verena*e n. comb. are closely related but are not sister taxa since *G. kathyae* n. sp. was recovered as the sister group to *G. verenae* n. comb. (Fig. 2). It would seem reasonable that the split between the *G. aristata* and the *G. kathyae* n. sp. / *G. verenae* n. comb. clade could be dated at around 30 mya.

Galapagomystides has been inferred to feed on the blood based on anatomical studies by Jenkins *et al.* (2002) though they could not identify the prey. They noted the presence of fine cuticular spines at the tip of the proboscis based on histology. Figure 8G shows an everted proboscis of *G. aristata* and there do appear to be fine spines at the everted tip. There have been several ecological studies associating *Galapagomystides* with Vestimentifera (Becker *et al.* 2013; Govenar *et al.* 2004; Govenar *et al.* 2005; Tsurumi and Tunnicliffe 2003; Govenar and Fisher 2007). There was a higher *G. aristata* concentration in real *Riftia pachyptila* tube assemblages when compared with the artificial tube assemblages, suggesting that *G. aristata* were there to feed on the real *Riftia pachyptila.* Further photo documentation (Fig. 14) of *Galapagomystides verenae* n. comb. atop juvenile *Escarpia spicata* tubes is provided here as well as *G. patricki* n. sp. living in dead vestimentiferan tubes (Fig. 19A). Contrary evidence to a blood diet for *Galapagomystides* has been provided in a stable isotope study (Bergquist *et al.* 2007) that showed *G. verenae* n. comb. had δ13C and δ15N values suggesting a diet containing the annelid *Nicomache venticola* Blake and Hilbig, 1990 and the gastropod *Depressigyra globulus* Warén and Bouchet, 1989. Both these proposed prey taxa lack external gills, feeding plumes or accessible features for blood feeding. Further study is needed to determine the actual prey of *Galapagomystides,* but we suggest that the current evidence points towards Vestimentifera.

Acknowledgements

Collections for this project were partly funded by the USA National Science Foundation (NSF) to Lisa Levin and GWR (OCE-0826254 and OCE-0939557, OCE-1634172) and by the Schmidt Ocean Institute. Many thanks to the captain and crew of the R/V *Atlantis*, R/V *Melville*, R/V *Western Flyer*, and R/V *Falkor* and the pilots of the HOV *Alvin* and ROVs *Jason* II, *Doc Ricketts* and *SuBastian* for crucial assistance in specimen collection. Specimens from Costa Rica were collected with permission of Instituto Costarricense de Pesca y Acuicultura (permit

INCOPESCA-CPI-003-12-2018) and Comisión Nacional para la Gestión de la Biodiversidad (permit R-070-2018-OT-CONAGEBIO). The authors are grateful to Chief Scientists Lisa Levin, Erik Cordes, Victoria Orphan and Bob Vrijenhoek. Jose Carvajal and Avery Hiley are thanked for help with DNA sequencing. Thanks also to Charlotte Seid (SIO-BIC) for dealing with cataloguing, along with Shirley Sorokin (SAMA). We thank an anonymous Reviewer, Patri Álvarez-Campos and the editor, Pat Hutchings, for their valuable comments on the manuscript.

References

Bandelt, H.J., Forster, P. & Röhl, A. (1999) Median-joining networks for inferring intraspecific phylogenies. *Molecular biology and evolution*, 16, 37–48.
https://doi.org/10.1093/oxfordjournals.molbev.a026036

Becker, E.L., Cordes, E.E., Macko, S.A., Lee, R.W. & Fisher, C.R. (2013) Using stable isotope compositions of animal tissues to infer trophic interactions in Gulf of Mexico lower slope seep communities. *PloS One* 8, e74459.
https://doi.org/10.1371/journal.pone.0074459

Bergquist, D.C., Eckner, J.T., Urcuyo, I.A., Cordes, E.E., Hourdez, S., Macko, S.A. & Fisher, C.R. (2007) Using stable isotopes and quantitative community characteristics to determine a local hydrothermal vent food web. *Marine Ecology Progress Series*, 330, 49–65.
https://doi.org/10.3354/meps330049

Blake, J.A. (1985) Polychaeta from the vicinity of deep-sea geothermal vents in the eastern pacific. I. Euphrosinidae, Phyllodocidae, Hesionidae, Nereididae, Glyceridae, Dorvilleidae, Orbiniidae, and Maldanidae. *Bulletin of the Biological Society of Washington*, 6, 67–101.

Blake, J.A. (1994) Family Phyllodocidae Savigny, 1818. *In:* Blake, J.A. & Hilbig, B. (Ed.), *Taxonomic Atlas of the Benthic Fauna of the Santa Maria Basin and Western Santa Barbara Channel. Vol. 4. The Annelida. Part 2*. Science Applications International Corporation, Woods Hole, pp. 115–86.

Blake, J.A. & Hilbig, B. (1990) Polychaeta from the vicinity of deep-sea hydrothermal vents in the eastern pacific. II. New Species and Records from the Juan de Fuca and Explorer Ridge Systems. *Pacific Science*, 44, 219–253

Borda, E., Kudenov, J.D., Chevaldonné, P., Blake, J.A., Desbruyères, D., Fabri, M.C., Hourdez, S., Pleijel, F., Shank, T.M., Wilson, N.G., Schulze, A. & Rouse, G.W. (2013) Cryptic species of *Archinome* (Annelida: Amphinomida) from vents and seeps. *Proceedings. Biological Sciences: The Royal Society*, 280, 20131876.
https://doi.org/10.1098/rspb.2013.1876

Carr, C.M., Hardy, S.M., Brown, T.M., Macdonald, T.A. & Hebert, P.D.N. (2011) A tri-oceanic perspective: DNA barcoding reveals geographic structure and cryptic diversity in Canadian polychaetes. *PloS One* 6, e22232.
https://doi.org/10.1371/journal.pone.0022232

Chapman, A.S.A., Tunnicliffe, V. & Bates, A.E. (2018) Both rare and common species make unique contributions to functional diversity in an ecosystem unaffected by human activities. *Diversity & Distributions*, 24, 568–78.
https://doi.org/10.1111/ddi.12712

Chevaldonné, P., Jollivet, D., Desbruyères, D., Lutz, R. & Vrijenhoek, R. (2002) Sister-species of eastern Pacific hydrothermal vent worms (Ampharetidae, Alvinellidae, Vestimentifera) provide new mitochondrial COI clock calibration. *Cahiers de Biologie Marine*, 43, 367–370.

Cordes, E.E., Carney, S.L., Hourdez, S., Carney, R.S., Brooks, J.M. & Fisher, C.R. (2007) Cold seeps of the deep Gulf of Mexico: Community structure and biogeographic comparisons to Atlantic equatorial belt seep communities. *Deep Sea Research Part I: Oceanographic Research Papers*, 54, 637–653.
https://doi.org/10.1016/j.dsr.2007.01.001

Darriba, D., Posada, D., Kozlov, A.M., Stamatakis, A., Morel, B. & Flouri, T. (2020) ModelTest-NG: a new and scalable tool for the selection of DNA and protein evolutionary models. *Molecular Biology and Evolution*, 37, 291–94. https://doi.org/10.1093/molbev/msz189

Desbruyères, D. & Segonzac, M. (1997) *Handbook of deep-sea hydrothermal vent fauna*. IFREMER, Brest, 279 pp.

Desbruyères, D., Segonzac, M. & Bright, M. (Eds.) (2006) *Handbook of deep-sea hydrothermal vent fauna*. Denisia, Linz, 5 pp.

Dreyer, J.C. (2004) Stability at hydrothermal-vent mussel beds: dynamics at hydrothermal vents: evidence for stable macrofaunal communities in mussel beds on the northern East Pacific Rise. MA from College of William and Mary. Available from: https://doi.org/10.21220/s2-e641-wn93 (accessed 5 April 2022)

Edler, D., Klein, J., Antonelli, A. & Silvestro, D. (2021) raxmlGUI 2.0: A graphical interface and toolkit for phylogenetic analyses using RAxML. *Methods in Ecology and Evolution*, 12, 373–77.
https://doi.org/10.1111/2041-210X.13512

Eklöf, J., Pleijel, F. & Sundberg, P. (2007) Phylogeny of benthic Phyllodocidae (Polychaeta) based on morphological and molecular data. *Molecular Phylogenetics and Evolution*, 45, 261–71.
https://doi.org/10.1016/j.ympev.2007.04.015

Giribet, G., Carranza, S., Baguna, J., Riutort, M. & Ribera C. (1996) First molecular evidence for the existence of a Tardigrada

Arthropoda clade. *Molecular Biology and Evolution*, 13, 76–84.
https://doi.org/10.1093/oxfordjournals.molbev.a025573.
Gollner, S., Govenar, B., Fisher, C.R. & Bright, M. (2015) Size matters at deep-sea hydrothermal vents: different diversity and habitat fidelity patterns of meio- and macrofauna. *Marine Ecology Progress Series*, 520, 57–66.
https://doi.org/10.3354/meps11078
Govenar, B.W., Bergquist, D.C., Urcuyo, I.A., Eckner, J.T. & Fisher, C.R. (2002) Three *Ridgeia piscesae* assemblages from a single Juan de Fuca Ridge sulphide edifice: structurally different and functionally similar. *Cahiers de Biologie Marine*, 43, 247–52.
Govenar, B.W., Freeman, M., Bergquist, D.C., Johnson, G.A. & Fisher, C.R. (2004) Composition of a one-year-old *Riftia Pachyptila* community following a clearance experiment: insight to succession patterns at deep-sea hydrothermal vents. *The Biological Bulletin*, 207, 177–82.
https://doi.org/10.2307/1543204
Govenar, B.W., Le Bris, N., Gollner, S., Glanville, J., Aperghis, A.B., Hourdez, S. & Fisher, C.R. (2005) Epifaunal community structure associated with *Riftia Pachyptila* aggregations in chemically different hydrothermal vent habitats. *Marine Ecology Progress Series*, 305, 67–77.
https://doi.org/10.3354/meps305067
Govenar, B.W. & Fisher, C.R. (2007) Experimental evidence of habitat provision by aggregations of *Riftia Pachyptila* at hydrothermal vents on the East Pacific Rise. *Marine Ecology*, 28, 3–14.
https://doi.org/10.1111/j.1439-0485.2007.00148.x
Hartman, O. (1936) A review of the Phyllodocidae (Annelida, Polychaeta) of the coast of California, with descriptions of nine new species. *University of California Publications in Zoology*, 41, 117–132.
Hatch, A.S., Liew, H., Hourdez, S. & Rouse, G.W. (2020) Hungry scale worms: phylogenetics of *Peinaleopolynoe* (Polynoidae, Annelida), with four new species. *ZooKeys*, 932, 27–74.
https://doi.org/10.3897/zookeys.932.48532
Imajima, M. (2001) Deep-sea benthic polychaetous annelids of Tosa Bay, southwestern Japan. *National Science Museum Monographs*, 20, 31–100.
Jenkins, C.D., Ward, M.E., Turnipseed, M., Osterberg, J. & Van Dover, C.L. (2002) The digestive system of the hydrothermal vent polychaete *Galapagomystides aristata* (Phyllodocidae): evidence for hematophagy? *Invertebrate Biology*, 121, 243–254.
https://doi.org/10.1111/j.1744-7410.2002.tb00064.x
Jimi, N., Kimura, T., Ogawa, A. & Kajihara, H. (2020) Alien worm in worm: a new genus of endoparasitic polychaete (Phyllodocidae, Annelida) from scale worms (Aphroditidae and Polynoidae, Annelida). *Systematics and Biodiversity*, 19, 13–21.
https://doi.org/10.1080/14772000.2020.1785038
Katoh, K. & Standley, D.M. (2013) MAFFT multiple sequence alignment software version 7: improvements in performance and usability. *Molecular Biology and Evolution*, 30, 772–80.
https://doi.org/10.1093/molbev/mst010
Kearse, M., Moir, R., Wilson, A., Stones-Havas, S., Cheung, M., Sturrock, S., Buxton, S., Cooper, A., Markowitz, S., Duran, C. & Thierer, T. (2012) Geneious basic: an integrated and extendable desktop software platform for the organization and analysis of sequence data. *Bioinformatics*, 28, 1647–49.
https://doi.org/10.1093/bioinformatics/bts199
Kelly, N., Metaxas, A. & Butterfield, D. (2007) Spatial and temporal patterns of colonization by deep-sea hydrothermal vent invertebrates on the Juan de Fuca Ridge, NE Pacific. *Aquatic Biology*, 1, 1–16.
https://doi.org/10.3354/ab00001
Kiel, S. (2016) A biogeographic network reveals evolutionary links between deep-sea hydrothermal vent and methane seep faunas. *Proceedings of the Royal Society B: Biological Sciences*, 283, 2016–2337.
https://doi.org/10.1098/rspb.2016.2337
Kobayashi, G. & Kojima, S. (2017) First record of *Protomystides hatsushimaensis* (Annelida: Phyllodocidae) inhabiting vacant tubes of vestimentiferan tubeworms. *Marine Biodiversity Records*, 10, 25.
https://doi.org/10.1186/s41200-017-0127-9
Kozlov, M.A., Darriba, D., Flouri, T., Morel, B. & Stamatakis, A. (2019) RAxML-NG: A fast, scalable, and user-friendly tool for maximum likelihood phylogenetic inference. *Bioinformatics*, 35, 4453–4455.
https://doi.org/10.1093/bioinformatics/btz305
Krylova, E.M. & Sahling, H. (2010) Vesicomyidae (Bivalvia): current taxonomy and distribution. *PloS One*, 5, e9957.
https://doi.org/10.1371/journal.pone.0009957
Le, H.L., Lecointre, G. & Perasso, R. (1993) A 28S rRNA-based phylogeny of the gnathostomes: first steps in the analysis of conflict and congruence with morphologically based cladograms. *Molecular Phylogenetics and Evolution*, 2, 31–51.
https://doi.org/10.1006/mpev.1993.1005
Leigh, J.W., Bryant, D. & Nakagawa, S. (2015) POPART: full-feature software for haplotype network construction. *Methods in Ecology and Evolution*, 6, 1110–1116.
https://doi.org/10.1111/2041-210X.12410

Leiva, C., Riesgo, A., Avila, C., Rouse, G.W. & Taboada, S. (2018) Population structure and phylogenetic relationships of a new shallow-water Antarctic phyllodocid annelid. *Zoologica Scripta*, 47, 714–26.
https://doi.org/10.1111/zsc.12313

Lelièvre, Y., Sarrazin, J., Marticorena, J., Schaal, G., Day, T., Legendre, P., Hourdez, S. & Matabos, M. (2017) Biodiversity and trophic ecology of hydrothermal vent fauna associated with tubeworm assemblages on the Juan de Fuca Ridge. *Biogeosciences Discussions*, 2017, 1–34.
https://doi.org/10.5194/bg-2017-411

Levin, L., Baco, A., Bowden, D., Colaco, A., Cordes, E., Cunha, M., Demopoulos, A., Gobin, J., Grupe, B., Le, J., Metaxas, A., Netburn, A., Rouse, G., Thurber, A., Tunnicliffe, V., Dover, C.V., Vanreusel, A. & Watling, L. (2016) Hydrothermal vents and methane seeps: Rethinking the sphere of influence. *Frontiers in Marine Science*, 3, 72.
https://doi.org/10.3389/fmars.2016.00072

Lewis, P.O. (2001) A likelihood approach to estimating phylogeny from discrete morphological character data. *Systematic Biology*, 50, 913–25.
https://doi.org/10.1080/106351501753462876

Lockyer, A.E., Olson, P.D. & Littlewood, D.T.J. (2003) Utility of complete large and small subunit rRNA genes in resolving the phylogeny of the Neodermata (Platyhelminthes): Implications and a review of the cercomer theory. *Biological Journal of the Linnean Society*, 78, 155–71.
https://doi.org/10.1046/j.1095-8312.2003.00141.x

Maddison, W.P. & Maddison, D.R. (2019) Mesquite: a modular system for evolutionary analysis. Version 3.61. Available from: http://www.mesquiteproject.org (accessed 28 September 2021)

McCowin, M.F., Feehery, C. & Rouse, G.W. (2020) Spanning the depths or depth-restricted: three new species of *Bathymodiolus* (Bivalvia, Mytilidae) and a new record for the hydrothermal vent *Bathymodiolus Thermophilus* at methane seeps along the Costa Rica Margin. *Deep Sea Research Part I: Oceanographic Research Papers*, 164, 103–322.
https://doi.org/10.1016/j.dsr.2020.103322

McCowin, M.F. & Rouse, G.W. (2018) A New *Lamellibrachia* species and confirmed range extension for *Lamellibrachia Barhami* (Siboglinidae, Annelida) from Costa Rica methane seeps. *Zootaxa*, 4504 (1), 1–22.
https://doi.org/10.11646/zootaxa.4504.1.1

Milligan, B.N. & Tunnicliffe, V. (1994) Vent and nonvent faunas of Cleft Segment, Juan de Fuca Ridge, and their relations to lava age. *Journal of Geophysical Research*, 99, 4777–4786.
https://doi.org/10.1029/93JB03210

Miura, T. (1988) A new species of the genus *Protomystides* (Annelida, Polychaeta) associated with a Vestimentiferan worm from the Hatsushima Cold-Seep site. *Japanese Society of Systematic Zoology*, 38, 10–14.

Muir, A. & Maruf Hossain, M.M. (2014) The intertidal polychaete (Annelida) fauna of the Sitakunda coast (Chittagong, Bangladesh), with notes on the Capitellidae, Glyceridae, Lumbrineridae, Nephtyidae, Nereididae and Phyllodocidae of the "Northern Bay of Bengal Ecoregion." *ZooKeys*, 419, 1–27.
https://doi.org/10.3897/zookeys.419.7557

Palumbi, S.R., Martin, A., Romano, S., McMillan, W.O., Stice, L. & Grabowski, G. (1991) *The simple fool's guide to PCR. Version 2.0*. University of Hawaii, Honolulu, 45 pp.

Peek, A.S., Gustafson, R.G., Lutz, R.A. & Vrijenhoek, R.C. (1997) Evolutionary relationships of deep-sea hydrothermal vent and cold-water seep clams (Bivalvia: Vesicomyidae): results from the mitochondrial cytochrome oxidase subunit I. *Marine Biology*, 130, 151–61.
https://doi.org/10.1007/s002270050234

Pleijel, F. (1991) Phylogeny and classification of the Phyllodocidae (Polychaeta). *Zoologica Scripta*, 20, 225–261.
https://doi.org/10.1111/j.1463-6409.1991.tb00289.x

Rodrigo, A.P., Costa, M.H., de Matos, A.P.A., Carrapiço, F. & Costa, P.M. (2015) A study on the digestive physiology of a marine polychaete (*Eulalia viridis*) through microanatomical changes of epithelia during the digestive cycle. *Microscopy and Microanalysis*, 21, 91–101.
https://doi.org/10.1017/S143192761401352X

Ronquist, F., Teslenko, M., Van Der Mark, P., Ayres, D.L., Darling, A., Höhna, S., Larget, B., Liu, L., Suchard, M.A. & Huelsenbeck, J.P. (2012) MrBayes 3.2: efficient Bayesian phylogenetic inference and model choice across a large model space. *Systematic Biology*, 61, 539–42.
https://doi.org/10.1093/sysbio/sys029

Rouse, G.W. & Kupriyanova, E.K. (2021) *Laminatubus* (Serpulidae, Annelida) from Eastern Pacific hydrothermal vents and methane seeps, with description of two new species. *Zootaxa*, 4915 (1), 1–27.
https://doi.org/10.11646/zootaxa.4915.1.1

Rouse, G.W. & Pleijel, F. (2003) Problems in polychaete systematics. *Hydrobiologia*, 496, 175–89.
https://doi.org/10.1023/A:1026188630116

Rouse, G.W., Pleijel, F. & Tilic, E. (2022) *Annelida*. Oxford University Press, London/New York, 418 pp.

San Martín, G., Álvarez-Campos, P., Kondo, Y., Núñez, J., Fernández-Álamo, M.A., Pleijel, F., Goetz, F.E., Nygren, A. & Osborn, K. (2021) New symbiotic association in marine annelids: Ectoparasites of comb jellies. *Zoological Journal of the Linnean Society*, 191, 672–694.

https://doi.org/10.1093/zoolinnean/zlaa034
Sibuet, M. & Olu, K. (1998) Biogeography, biodiversity and fluid dependence of deep-sea cold-seep communities at active and passive margins. *Deep-Sea Research. Part II, Topical Studies in Oceanography*, 45, 517–67.
https://doi.org/10.1016/S0967-0645(97)00074-X
Smith, C.R. & Baco, A.R. (1998) Phylogenetic and functional affinities between whale-fall, seep and vent chemoautotrophic communities. *Cahiers de Biologie Marine*, 39, 345–346.
Solís-Weiss, V. & Hernández-Alcántara, P. (1994) *Amphisamytha fauchaldi*: a new species of ampharetid (Annelida: Polychaeta) from the hydrothermal vents at Guaymas Basin, Mexico. *Bulletin of the Southern California Academy of Sciences*, 93, 127–134.
Stamatakis, A. (2014) RAxML version 8: A tool for phylogenetic analysis and post-analysis of large phylogenies. *Bioinformatics*, 30, 1312–1313.
https://doi.org/10.1093/bioinformatics/btu033
Stiller, J., Rousset, V., Pleijel, F., Chevaldonné, P., Vrijenhoek, R.C. & Rouse, G.W. (2013) Phylogeny, biogeography and systematics of hydrothermal vent and methane seep *Amphisamytha* (Ampharetidae, Annelida), with descriptions of three new species. *Systematics and Biodiversity*, 11, 35–65.
https://doi.org/10.1080/14772000.2013.772925
Tsurumi, M. & Tunnicliffe, V. (2003) Tubeworm-associated communities at hydrothermal vents on the Juan de Fuca Ridge, Northeast Pacific. *Deep Sea Research Part I: Oceanographic Research Papers*, 50, 611–29.
https://doi.org/10.1016/S0967-0637(03)00039-6
Tunnicliffe, V. (1992) The nature and origin of the modern hydrothermal vent fauna. *Palaios*, 7, 338–2350.
https://doi.org/10.2307/3514820
Tunnicliffe, V., Juniper, S.K. & Sibuet, M. (2003) Reducing environments of the deep-sea floor. *In*: Tyler, P.A. (Ed.), *Ecosystems of the world. 28. Ecosystems of the Deep Oceans*. Elsevier, Amsterdam, pp. 81–110.
Tunnicliffe, V., McArthur, A.G. & McHugh, D. (1998) A biogeographical perspective of the deep-sea hydrothermal vent fauna. *Advances in Marine Biology*, 34, 353–442.
https://doi.org/10.1016/S0065-2881(08)60213-8
Tyler, P.A., German, C.R., Ramirez-Llodra, E. & Van Dover, C.L. (2002) Understanding the biogeography of chemosynthetic ecosystems. *Oceanologica Acta*, 25, 227–241.
https://doi.org/10.1016/S0399-1784(02)01202-1
Vaidya, G., Lohman, D.J. & Meier, R. (2011) SequenceMatrix: concatenation software for the fast assembly of multi-gene datasets with character set and codon information. *Cladistics*, 27, 171–180.
https://doi.org/10.1111/j.1096-0031.2010.00329.x
Van Dover, C. (2000) *The Ecology of Deep-sea Hydrothermal Vents*. Princeton University Press, Princeton, New Jersey, 424 pp.
Van Dover, C.L. (2002) Community structure of mussel beds at deep-sea hydrothermal vents. *Marine Ecology Progress Series*, 230, 137–158.
https://doi.org/10.3354/meps230137
Warèn, A. & Bouchet, P. (1989) New gastropods from East Pacific hydrothermal vents. *Zoologica Scripta*, 18, 67–102.
https://doi.org/10.1111/j.1463-6409.1989.tb00124.x
Watanabe, H., Fujikura, K., Kojima, S., Miyazaki, J.I. & Fujiwara, Y. (2010) Japan: vents and seeps in close proximity. *In:* Kiel, S. (Ed.), *The Vent and Seep Biota. Vol. 33. Aspects from Microbes to Ecosystems*. Springer, Dordrecht, pp. 379–401.
https://doi.org/10.1007/978-90-481-9572-5_12
Whiting, M.F., Carpenter, J.C., Wheeler, Q.D. & Wheeler, W.C. (1997) The Strepsiptera problem: phylogeny of the holometabolous insect orders inferred from 18S and 28S ribosomal DNA sequences and morphology. *Systematic Biology*, 46, 1–68.
https://doi.org/10.1093/sysbio/46.1.1
Wolff, T. (2005) Composition and endemism of the deep-sea hydrothermal vent fauna. *Cahiers de Biologie Marine*, 46, 97–104.
Yen, N.K. & Rouse, G.W. (2020) Phylogeny, biogeography and systematics of Pacific vent, methane seep, and whale-fall *Parougia* (Dorvilleidae: Annelida), with eight new species. *Invertebrate Systematics*, 34, 200–233.
https://doi.org/10.1071/IS19042.